FINAL REPORT

NASA INNOVATIVE RESEARCH PROGRAM (IRP)
NASA GRANT - NAGW-1601

ARTIFICIAL INTELLIGENCE FOR GEOLOGIC MAPPING WITH IMAGING SPECTROMETERS

Center for the Study of Earth from Space (CSES)
Cooperative Institute for Research in Environmental Science (CIRES)
University of Colorado, Boulder, CO 80309-0449

P. I. - F. A Kruse
Period of performance - 02/01/89 to 01/31/93
Report date: 29 January 1993

ARTIFICIAL INTELLIGENCE FOR GEOLOGIC MAPPING WITH IMAGING SPECTROMETERS

Center for the Study of Earth from Space (CSES), Cooperative Institute for Research in Environmental ScienceS (CIRES),University of Colorado, Boulder, CO 80309-0449
P. I. - F. A Kruse
29 January 1993

EXECUTIVE SUMMARY - FINAL REPORT

This project was a three year study at the Center for the Study of Earth from Space (CSES) within the Cooperative Institute for Research in Environmental Science (CIRES) at the University of Colorado, Boulder. The research was funded by the NASA Innovative Research Program (IRP) NAGW-1601. The goal of this research was to develop an expert system to allow automated identification of geologic materials based on their spectral characteristics in imaging spectrometer data such as the Airborne Visible/Infrared Imaging Spectrometer (AVIRIS). This requirement was dictated by the volume of data produced by imaging spectrometers, which prohibits manual analysis. The research described here is based on the development of automated techniques for analysis of imaging spectrometer data that emulate the analytical processes used by a human observer. The research tested the feasibility of such an approach, implemented an operational system, and tested the validity of the results for selected imaging spectrometer data sets. Notable results of the research include:

1) Development of a prototype spectral database in conjunction with International Geologic Correlation Program (Project IGCP-264, "Remote Sensing Spectral Properties"). The database consists of reflectance spectra measured on 5 spectrometers for 26 common minerals with supporting analytical information. The spectra have already been released in digital form and results are also being published by the American Geophysical Union (AGU) for international distribution.

2) Development of automated techniques for the extraction and characterization of absorption features in field, laboratory, and aircraft reflectance spectra. Individual spectra are analyzed in terms of the position of absorption features, their depth, width, and shape.

3) Implementation of a prototype expert system and successful testing on individual laboratory, field, and Airborne Visible/Infrared Imaging Spectrometer (AVIRIS) spectra.

4) Development of prototype visualization and analysis software for imaging spectrometer data; the "Spectral Image Processing System (SIPS)" version 1.0. SIPS has been adopted by CSES and over 75 organizations worldwide as the standard for imaging spectrometer data analysis. Further development, maintenance, and support has been turned over to CSES staff. CSES recently released SIPS version 1.2 for general use.

5)   Integration of the expert system into the image processing environment as the "General Use Expert System for Spectra (GUESS)" module to SIPS. This is a stand-alone software module for expert system analysis of imaging spectrometer data. It includes utilities for feature extraction, rule specification, expert system analysis of single spectra or entire imaging spectrometer data sets, and analysis and visualization of expert system results. GUESS has been tested on several AVIRIS scenes. The GUESS software will be released with full documentation as part of SIPS version 2.0 during 1993.

The digital absorption feature extraction and the expert system have been used successfully to analyze lab and field spectra of unknown minerals and individual spectra from imaging spectrometer data. They have been used to analyze entire AVIRIS images (~300,000 spectra per scene) resulting in automatic compilation of image maps showing the predominant surface mineralogy for use in detailed geologic studies. At one test site, the expert system analysis of the AVIRIS data is playing a major role in mapping lithological variation, and in conjunction with field mapping, in determining the spatial relations between lithology and faulting. The expert system results form the starting point for detailed quantitative analysis using other techniques that require spectral endmembers (such as spectral unmixing).

This research has resulted in an operational expert system prototype and supporting software. Some of the software is already being used internationally and is making positive impacts on the way organizations are analyzing imaging spectrometer data. The expert system software itself is being used internally for both student research and to support other projects, and will be released externally with full documentation during 1993. Published papers summarizing research results are listed in Appendix A.

TABLE OF CONTENTS

I. BACKGROUND

INTRODUCTION

Laboratory and field studies of the visible and near-infrared spectral properties of rocks and minerals have shown that many individual mineral species can be identified based on their spectral characteristics. The exact positions and shapes of visible and infrared absorption bands (low points in the spectral curves) are different for different minerals and reflectance spectra allow direct identification (Figure 1). Some of these characteristic spectral features are tabulated in the literature (Hunt et al., 1971; Hunt, 1977, 1979; Hunt and Ashley, 1979; Lee and Raines, 1984; Clark et al, 1990), however, the published data was largely collected using analog equipment and only recently have digital reflectance spectra become available (Clark et al., 1990; Grove and Hook, 1992; Kruse and Hauff, 1993).

With the advent of imaging spectrometers during the 1980s, it was obvious that the spectral properties of rocks, minerals, and vegetation, were not well understood, particularly in their natural settings. Imaging spectrometers measure reflected visible and infrared light utilizing many narrow contiguous spectral bands to construct detailed reflectance spectra for millions of discrete picture elements (pixels) (Goetz et al., 1985). Analysis of a single imaging spectrometer data set presented researchers with more reflectance spectra than they would normally see in an entire career. It was clear that basic spectral information was required to allow analysis of these data, and that new research was necessary to establish the foundations on which to build imaging spectrometer analysis capabilities. Although readily available published analog data had served as reference material for early geologic remote sensing efforts, new instrumentation, broadening research interests, and digital analysis capabilities mandated that new approaches to data collection, storage, and analysis be developed. The immense volume of data collected by these systems prohibited detailed manual analysis. The research reported here concentrated on developing automated techniques for digital analysis of imaging spectrometer data that emulate the analytical processes used by a human observer.

OBJECTIVES

The primary objectives of this work were to develop a knowledge base and an expert system approach for analysis of imaging spectrometer data. The main science objective was to characterize and map Earth surface materials based on their spectral properties in order to develop a better understanding of their surface distribution and relationship to geologic processes.

II. METHODS

GENERAL APPROACH

There were two aspects to this research. The first requirement was to develop a basic understanding of the spectral properties of Earth surface materials (the knowledge base). Although much work has been done for rocks and minerals, there was no comprehensive high spectral resolution digital database available, mineral

Figure 1. - Stacked reflectance spectra for selected minerals. Absorption features near 1.4 and 2.3 μm in co2004 (calcite) and cod2005 (dolomite) are caused by CO_3. Features near 2.2 μm in kl500, al705, and il107 (kaolinite, alunite, and muscovite) are caused by AL-OH bonds. Broad features near 0.9 μm in Fe2602 (hematite) and fe2600 (goethite) are caused by Fe^{3+}. Spectra are offset for clarity. Reference reflectance is given at 1.6 μm.
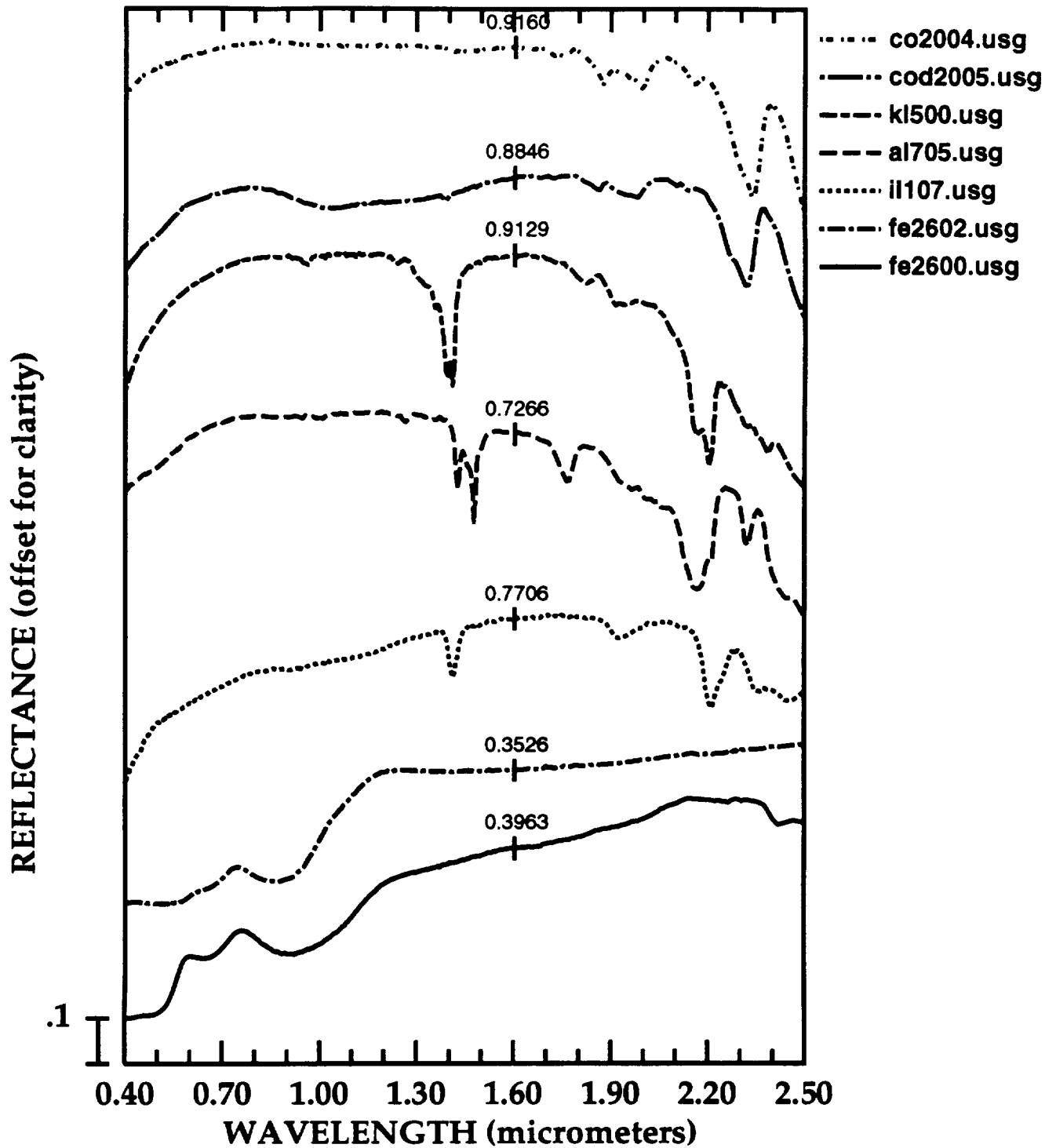
variation was not documented, and mixing was poorly understood. As part of this research, we systematically collected and measured pure mineral standards, rocks, and soils (Kruse and Hauff, 1993). The minerals standards used for the spectral database were also characterized using X-ray diffraction (XRD), scanning electron microscopy (SEM), and energy dispersive X-ray analysis (EDX). Basic spectral knowledge bases, of which this is one of the first, are necessary to allow quantitative analysis of laboratory, field, and imaging spectrometer data.

The second aspect of the research was to integrate the information derived from spectral databases with the imaging spectrometer data using an expert system approach. This work emphasized automatic extraction and characterization of spectral features from laboratory reflectance spectra, development of facts and rules based on an experienced analyst's interpretation of spectra, analysis of imaging spectrometer data based on the rules, and presentation of the results in image map format. As part of this research, we developed the interface, display, and analysis link between spectral libraries and high spectral resolution remote sensing. We used AVIRIS data and Geophysical and Environmental Research imaging spectrometer (GERIS) data for sites of geologic interest to the principal investigator to develop and test the image processing procedures.

SPECTRAL LIBRARY COMPILATION

High quality spectral libraries are the key to successful analysis of earth-surface materials using reflectance spectroscopy. The detail and accuracy of these analyses are limited by the extent and quality of the spectral library. The initial step in this research, therefore, was to compile a spectral library for common geologic materials. Materials selected for inclusion in the initial library were chosen because they were considered to be of major importance by respondents to an international survey conducted during 1988 as part of an UNESCO-sponsored project (International Geologic Correlation Program, Project IGCP-264 "Remote Sensing Spectral Properties"). The concept was to provide reflectance spectra for common geologic materials and to insure that these spectra were representative by characterizing the minerals using multiple analytical techniques. Each sample (26 total) was measured on a Beckman UV5270 spectrophotometer at CSES, a Beckman UV5240 spectrophotometer at the U.S. Geological Survey in Denver (Clark et al., 1990), on the "RELAB" spectrometer at Brown University (Pieters, 1990), on the "SIRIS" field spectrometer in the laboratory at CSES (Geophysical and Environmental Research, 1988) and with the prototype of a new high resolution field spectrometer, the "PIMA II" (manufactured by Integrated Spectronics Pty. Ltd.). These examples were chosen to show the effect of instrumentation and resolution on the reflectance spectra. The IGCP-264 spectral library provides the basic information for the expert system in the form of spectral features for specific materials. For each mineral included in the data base, the following information was compiled; summary information for each mineral, visible and infrared spectroscopy, X-Ray Diffraction (XRD) (including comparison to JCPDS standards) (JCPDS, 1974, 1980), Scanning Electron Microscopy (SEM), and Energy Dispersive X-ray chemistry (EDX). These reflectance spectra have already been released in digital form and the reflectance spectra and compiled analytical results are also being published by the American Geophysical Union (AGU) for international distribution (Kruse and Hauff, 1993).

EXPERT SYSTEM METHODOLOGY
Extracting and Characterizing Spectral Features

This research used numerical analysis and characterization of digital reflectance measurements to establish quantitative criteria for identifying minerals and mineral mixtures. The absorption feature information was extracted from each spectrum using the following automated techniques (Kruse et al., 1988, 1993; Kruse, 1990a, 1990b; Kruse and Lefkoff, 1993).

Continuum removal (Clark and Roush, 1984) was the first step of the feature extraction process used to characterize individual absorption features contained in a spectrum. The continuum of a spectrum, as used in this research, is a continuous, convex hull draped over the source spectrum at its high points (Figure 2). The continuum is computed by first locating all of the high points. Starting from the left-most high point, the program considers a straight line from this high point to the next high point along the spectrum with a greater or equal reflectance value. If this line does not cross the spectrum, the line segment connecting the two points is added to the continuum. If the line segment crosses the spectrum, then the program recursively backs up one point at a time, right to left, until the connecting line segment does not cross the spectrum. This new point is then added to the high point list and the program continues. Once the program crosses the highest reflectance point in the spectrum, the next connecting segment is considered with the largest remaining high point with a lower reflectance value than the previous high point. This method assures that the resulting continuum is always convex and does not cross through the original spectrum.

Dividing the source spectrum by its continuum spectrum results in a continuum-removed spectrum containing normalized reflectance values from 0.0 to 1.0 (Figure 2). Absorption features, which commonly occur superimposed on a background slope in the source spectrum, are transformed into features with a uniform, flat background of 1.0 in the continuum-removed spectrum. This allows each absorption feature in a spectrum to be mathematically analyzed with respect to a consistent reference plane.

Within one of the extracted features, a number of low points may occur in the continuum-removed spectrum. Four spectral attributes are defined for each of these low points (Figures 3 and 4). The position attribute is defined as the wavelength of the low point. The depth attribute is 1.0 (the continuum) minus the reflectance of the low point. The full-width-half-maximum (FWHM) attribute is the width of the feature at half of the depth. The asymmetry attribute, a simplistic measure of band shape that reduces description to one parameter, is the base ten logarithm of the area of the feature occurring to the right of the low point divided by the area of the feature to the left of the low point. Asymmetry then becomes zero if the band is symmetrical, negative if it is asymmetrical to the left, and positive if it is asymmetrical to the right (Figure 4).

Defining Critical Absorption Features

For the spectral library described above, each material (26 minerals total, plus green and dry vegetation) was analyzed using the continuum removal/feature extraction process and the four attributes (position, depth, FWHM, and asymmetry) were calculated for each of the low points in the continuum-removed spectrum. The "Facts" considered by the human expert to develop rules for analysis of

4

Figure 2. Example of the continuum and the continuum-removed spectrum for the mineral kaolinite (From Kruse and Lefkoff, 1992).

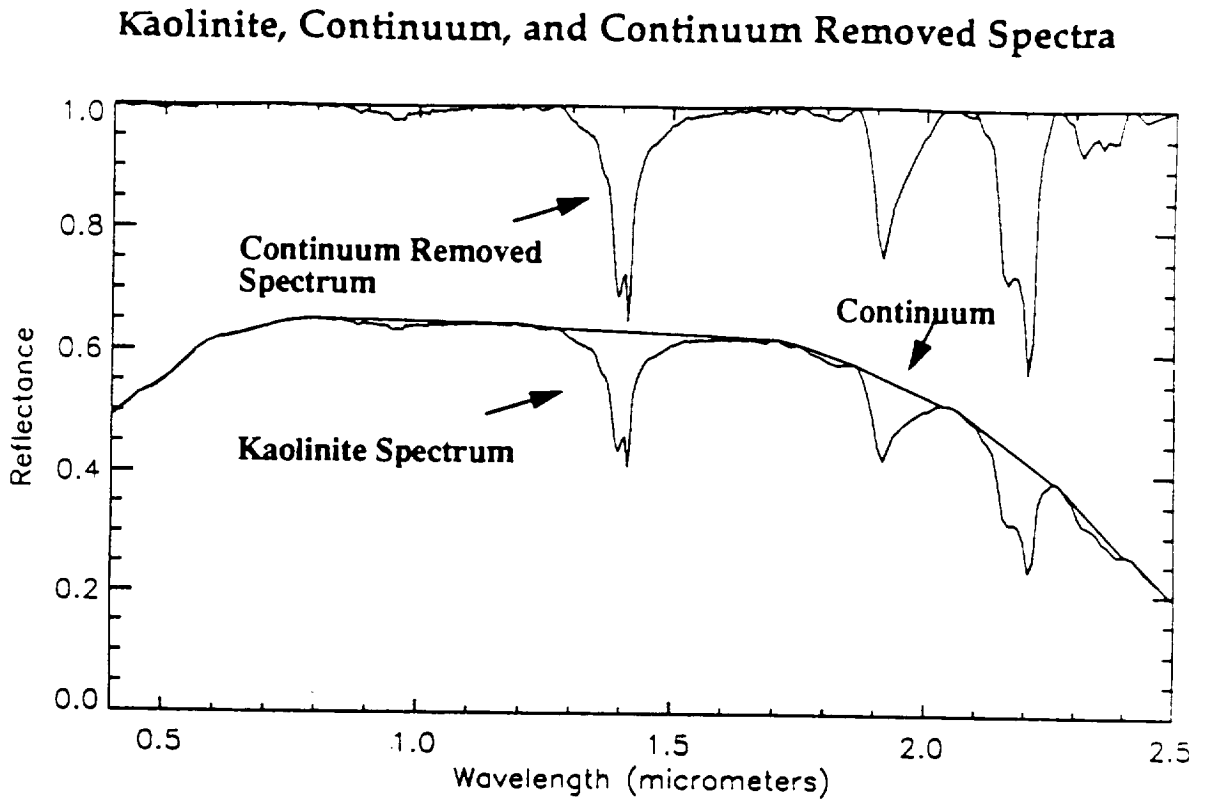## Kaolinite, Continuum, and Continuum Removed Spectra

Figure 3.   Plot showing the absorption band attributes position, depth, and full-width-half-maximum (FWHM) (From Kruse and Lefkoff, 1992).
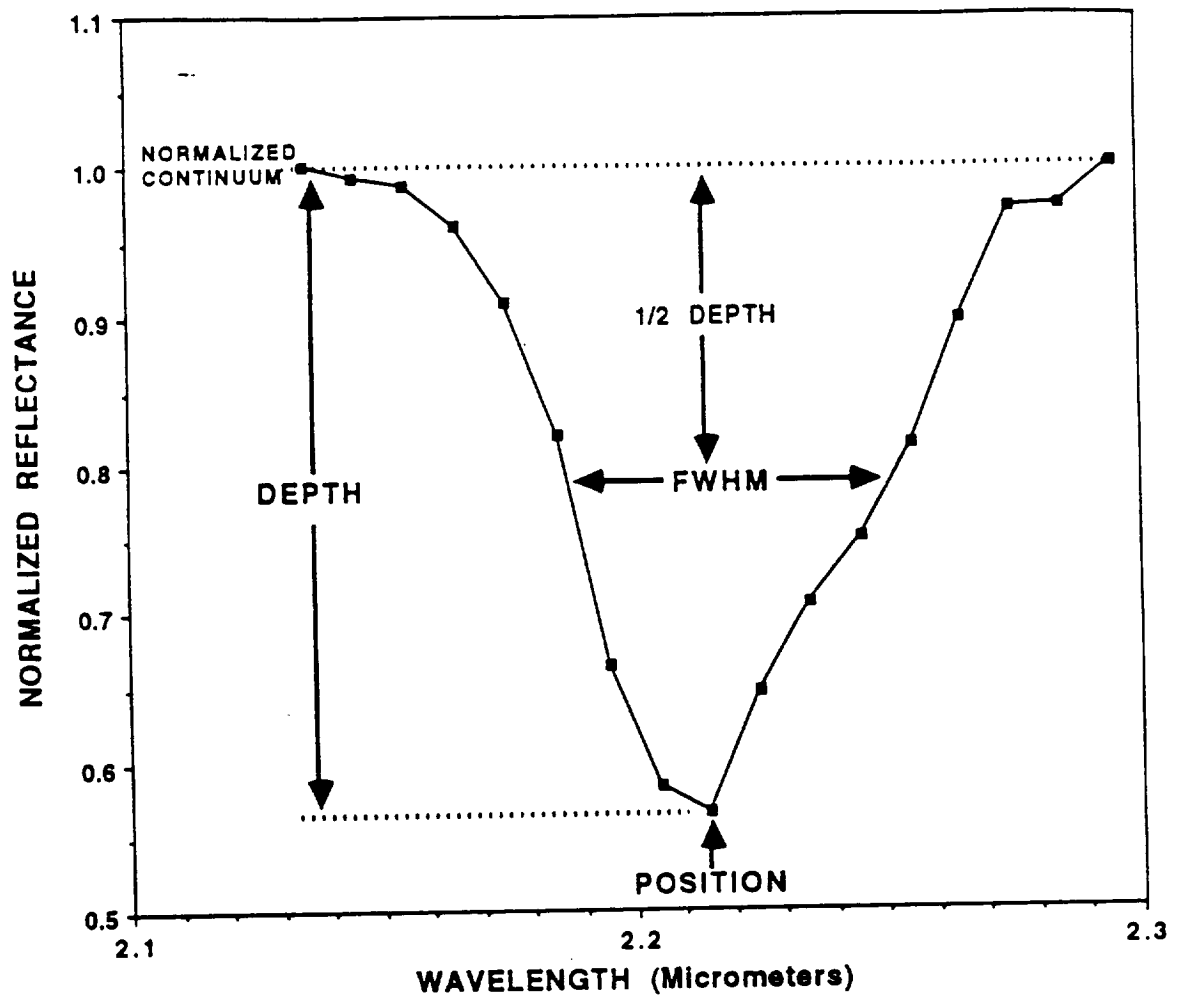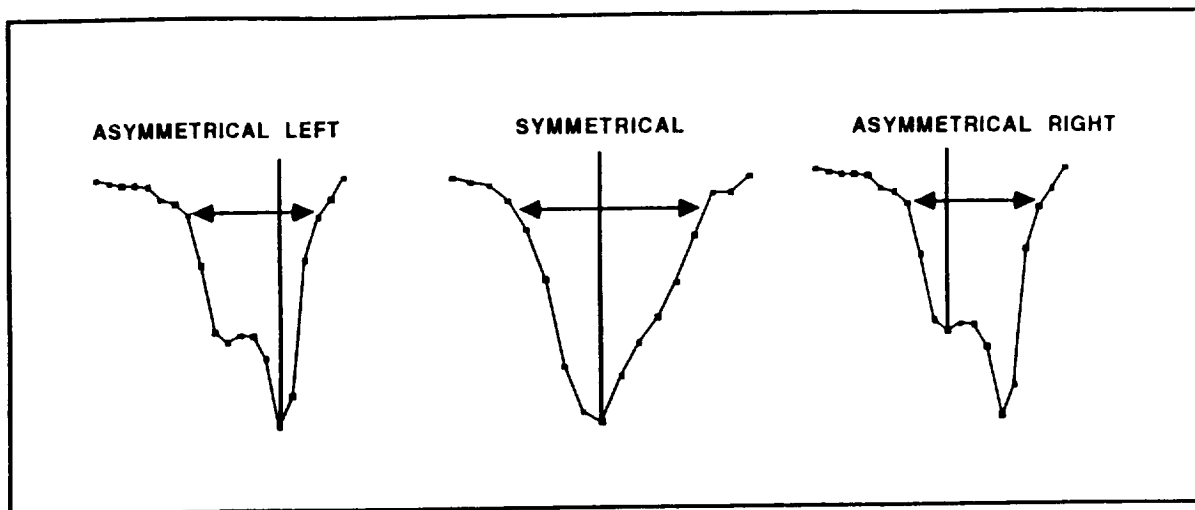
Figure 4.   Schematic showin the absorption band attribute asymmetry. Note the distribution of the areas to the left and right of the selected absorption minimum (From Kruse and Lefkoff, 1992).

unknown spectra consist of all of the spectral feature attributes for every feature identified during the analysis (Table 1).

The next step is for a knowledgeable user to determine which of these facts are characteristic of a particular material and best uniquely characterize the spectrum. These selections are made interactively based upon knowledge and information derived from experience. Much of this information is acquired through analysis of large numbers of reflectance spectra and from information published in the literature (Hunt, 1977; Hunt and Salisbury, 1970, 1971: Hunt et al., 1971; Lee and Raines, 1984; Clark et al., 1990; Grove et al., 1992; Kruse and Hauff, 1993). Figure 5 shows the interactive rule selection screen within the program "SFW" consisting of the fact table and the corresponding spectrum with features marked. In this case kaolinite is selected and displayed. The expert user determines which attributes of each fact are relevant and assigns comparison tolerances to each chosen attribute. Tolerances are based on the expert's knowledge of spectral variance. Entire facts can be selected or deselected. If a feature is deselected, the corresponding feature marker on the spectrum disappears, thus the expert gets visual feedback on his choices. Additionally, the attributes themselves are fully editable. The chosen facts become individual "rules" to be used by the expert system. The expert user assigns a relative weight to each rule based on its importance for identifying the material. Weights range from 0.0 (feature not required for identification) to 1.0 (feature mandatory for identification) and are assigned based upon the expert's knowledge of the spectral properties of materials.

Once the rules are built, then the expert system can be used to analyze unknown spectra. An input spectrum is compared to each spectrum in the library (endmember spectrum) to determine degree of match. Two different types of comparisons are used; binary encoding matching and feature matching to the rules described above. The binary encoding is added primarily to deal with spectrum noise and is particularly important when trying to analyze aircraft spectra, which tend to be much noisier than laboratory spectra.

Binary encoding is a matching technique in which the average of all spectral channels is determined and then each value is compared to the mean to determine if it is above or below the mean (Mazer et al., 1988). Individual values lower than the mean are assigned the value zero, while individual points above the mean are assigned the value one. The binary encoded unknown spectrum is compared point by point to the binary encoded endmember. The result is a value between 0.0 and 1.0 representing the number of points at which the encoded values match, presented as a percent match of the two encoded spectra.

The second comparison method applies the continuum removal/feature extraction algorithm to the unknown spectrum. The facts extracted from the unknown spectrum are compared to the rules for each endmember spectrum in the library to determine how many of the facts match the rules. A match occurs when all of the attributes of a fact from the input spectrum fall within the user defined tolerances of a rule's attributes. The result of the rule-based matching is a value between 0.0 and 1.0 corresponding to the sum of the weights of the matching rules divided by the sum of the weights of all of the rules for the selected endmember. For example, if a specific mineral was expected to have three absorption features and the expert user specifies that it must have one of the features, should have the second, and might have the third to be identified, then these three features could be

Table 1. FACT TABLE FOR SEVERAL MINERALS

Position	Depth	FWHM	Asymmetry
ALUNITE_K_al705 (Potassium Alunite)			
2.16500	0.37318	0.10219	-0.10095
2.21500	0.26392	0.11628	-1.16594
2.03500	0.05409	0.23566	1.36317
2.01500	0.04456	0.23869	1.70167
1.47900	0.29062	0.01679	-0.36046
1.42900	0.19506	0.01895	0.73380
2.32500	0.16622	0.03024	-0.18854
2.41800	0.16472	0.07263	0.05584
1.76400	0.12116	0.04991	-0.14785
ALUNITE_Na_al706 (Sodium Alunite)			
2.17500	0.35612	0.09881	-0.21739
2.21500	0.23707	0.13305	-0.91083
2.01500	0.06008	0.25634	1.37395
1.96500	0.01226	0.30067	2.47355
1.49800	0.20735	0.03120	-0.42705
1.43900	0.17779	0.02339	0.64841
1.57100	0.01066	0.20000	-1.65978
2.32500	0.17091	0.03303	0.01244
1.76400	0.14757	0.05292	-0.15998
2.44000	0.14594	0.08888	-0.13573
2.40000	0.11199	0.09679	0.70296
BUDDINGTONITE_nhb2301			
2.12500	0.25769	0.22012	0.04708
2.19500	0.17399	0.26053	-0.52084
2.05500	0.15166	0.27398	0.61666
2.01500	0.14873	0.27505	1.07181
2.30500	0.03623	0.38287	-1.53978
1.55800	0.02821	0.06986	0.36430
1.57100	0.02648	0.07260	0.13374
1.64000	0.01275	0.13998	-0.69283
1.61200	0.01260	0.14024	-0.37493
1.90500	0.02284	0.02600	-0.16291
1.41300	0.02163	0.02163	-0.14176
0.48500	0.01378	0.03755	0.08616
0.48900	0.01273	0.03826	-0.09337
0.49900	0.01193	0.03879	-0.56465
0.49500	0.01153	0.03905	-0.35206
0.47900	0.01013	0.04030	0.32356
KAOLINITE_W_XSTAL_kl500			
2.20500	0.32452	0.07185	-0.54577
2.16500	0.25838	0.07711	0.33188
2.09500	0.02138	0.15539	1.78273
1.41300	0.31686	0.04395	-0.44953
1.39800	0.29228	0.04664	-0.11524
1.35900	0.12928	0.11835	0.43102
1.46900	0.03096	0.23356	-1.19834
1.23800	0.02490	0.03691	1.72672
2.38600	0.05952	0.02403	-0.51408
2.35500	0.03045	0.04823	0.82100
1.91500	0.04801	0.05605	0.11757
2.31500	0.04327	0.04390	-0.35566

9

Figure 5. Unix screen dump of the rule selection tool for library spectra. Shown are the mineral selection menu (upper left), the spectral plot of the selected mineral kaolinite showing the positions of the absorption features marked with arrows (upper right), and the attribute selection menu allowing selection of important absorption band attributes and weghting of rules (bottom).

assigned respective weights of 1.0, 0.6, and 0.3 to differentiate their importance. If an unknown material only had two of the expected features (say the 1.0 and the 0.3 features) then the probability of occurrence of that specific mineral could be represented as (1.0+0.3)/(1.0 + 0.6 + 0.3) = 0.68. Note that this is not a true probability, but an empirical one used for decisions regarding relative certainty of identification; a "certainty probability".

In practice, particularly with noisy data, it is necessary to combine the binary results and the rule-based results to accurately identify materials. The final match for each endmember spectrum is calculated by weighting the binary and the rule-based results with fixed weights summing to 100% defined by the user. In the typical imaging spectrometer (AVIRIS) case, based upon evaluation of the data and comparison of single pixel spectra to library spectra, the binary results are weighted at 40% and the feature results at 60%. The user can also select other weighting factors depending on the quality of the data; noise-free data would ideally use only the absorption feature rules (weight of 100% assigned to the rules). Extremely noisy data could potentially use only the binary encoding algorithm (weight of 100% assigned to the binary encoding). The result of the weighted decision is a certainty probability between 0.0 and 1.0 describing how certain the expert system is that the given input spectrum matches a given endmember spectrum. A certainty of 1.0 indicates that all rules were satisfied and the binary encoding match was perfect.

III.   RESULTS

GENERAL

The expert system was operational for single spectra prior to the start of NASA funding in 1989, however, limited resources prevented implementation or optimization for imaging spectrometer data. The original expert system ran under the VAX VMS operating system on DEC MICROVAX computers. The feature extraction algorithms were coded in FORTRAN, while the expert itself was coded in the PROLOG programming language. The original expert system had a limited set of facts and rules and critical absorption band characteristics were not well defined. Once rules were defined, they were difficult to update or change.

Significant progress was made over the first year of the project, particularly in the area of spectral library compilation. A suite of spectra for "pure" minerals and several vegetation types and vegetation component spectra were analyzed to determine critical absorption bands for identification. This information was manually entered into a knowledge base for use by the expert system. Additional high resolution spectra (3.8 nm resolution, 1 nm sampling) were measured for 26 minerals. The mineralogy of these samples was well characterized using X-ray diffraction and Scanning Electron Microscopy. These results have been released in digital form and results are also being published by the AGU for international distribution (Kruse and Hauff, 1993).

During 1989 we also examined the spectral characteristics of vegetation. Spectra were obtained for vegetation components, different vegetation types, and vegetation under varying degrees of stress. The component spectra and the differences between green and dry vegetation were analyzed using the feature extraction procedures. The absorption band parameters for these materials were

entered into the knowledge base and facts and rules were utilized in the expert system to differentiate between minerals and vegetation, and between dry and green vegetation.

We also conducted a preliminary evaluation of vegetation spectra for quantification of biochemical variation. Results of a study of spectra from ozone-damaged Ponderosa Pine showed a correlation of $R^2=0.985$ between chlorophyll content and the depth of the 0.67 μm absorption feature and $R^2=0.83$ between chlorophyll content and the 0.67 μm band width (Singhroy and Kruse, 1991).

During 1989-1990, the expert system was recoded into the C programming language for portability and speed. We also looked at quantification of mineralogical variation using the absorption band characteristics. Our first comparisons were for a suite of illites from around the world (Kruse and Hauff, 1989; Hauff and Kruse, 1990; Kruse and Hauff, 1991), and of mixed layer kaolinite/smectites from the Paris Basin, France (Hauff and Kruse, 1990; Hauff et al., 1990; Kruse et al., 1991). The results demonstrate that the absorption band attributes can be used to quantify mineralogical variation. The kaolinite example in particular showed a strong linear relation between the asymmetry of the 2.2 μm absorption feature and the percent kaolinite vs smectite in the mixed layered clays (Kruse et al., 1991).

Additional research during 1990 consisted primarily of refinement and testing of the rules for the expert system and preliminary implementation of full dataset imaging spectrometer analysis using the expert system. We also added additional materials to the spectral database. We concentrated on collection of additional high resolution spectra (including some for multiple samples illustrating spectral variation) and supplemental data for the spectral database. We extracted and analyzed spectral features from the high spectral resolution spectra and used this information to refine rules. We continued to measure and quantify spectral variation using laboratory instrumentation and digital analysis. Additional samples were measured that illustrated the quantification of kaolinite layers in mixed-layer kaolinite/smectite clays. We also conducted field testing of the quantitative spectrum analysis procedures, confirming the validity of the method on in-situ rocks and soils and establishing reproducibility of the estimates to 5-10% (Kruse et al., 1991). We also analyzed spectra of stressed vegetation from the Canadian boreal forest and reaffirmed the very strong relationship between decreased absorption band depth and width (FWHM) at 0.67 μm and stress in vegetation, in this case caused by the presence of heavy metals (Singhroy and Kruse, 1991).

During 1991 and a no-cost extension into 1992 we implemented the feature analysis procedures developed for analysis of the individual spectra for use on entire imaging spectrometer data sets, typically containing over 300,000 pixels (spectra). This included refinement of the continuum removal procedures to deal with noisy data and improved feature extraction and feature characterization procedures. All software was converted to the "Interactive Data Language (IDL)" (RSI, 1992) and "C" running on UNIX platforms. The "Spectral Image Processing System (SIPS)" was designed and implemented, initially to view expert system results. During late 1991 SIPS was turned over to CSES programming staff and released externally as an operational system to support general imaging spectrometer research and analysis. The 1992 no-cost-extension was also used to implement the expert system using IDL, to document the software, and to conduct

12

expert system analyses of AVIRIS and/or GERIS image data from several areas in Nevada, California, and Utah (Kruse, 1992a, 1992b; Kruse and Lefkoff, 1992, 1993; Kruse et al., 1993a).

CHARACTERIZATION OF MATERIALS
IGCP SPECTRAL DATABASE

International Geological Correlation Project (IGCP) # 264 (Remote Sensing Spectral properties) sponsored by UNESCO was formed in 1987 to address some of the questions arising from developments in the field of imaging spectrometry, and analysis of spectral reflectance data in general. Under the direction of the PI who acted as database committee chairman, a questionnaire on spectral database requirements was initially sent out in November of 1987, in January of 1988 and in August of 1988 to an international group of about scientists. Responses were used to compile statistics on database requirements for geologic applications. This information was distributed to all IGCP-264 participants in the report of the 1988 meeting. The materials in Table 2 were listed in this report as the most important for geologic applications of spectral remote sensing. Subsequently, as many as possible of these were used in the initial compilation of minerals for inclusion in the IRP expert system study.

TABLE 2.   COMMON MATERIALS OF INTEREST TO GEOSCIENTISTS

Amphiboles
    ACTINOLITE
    TREMOLITE
Carbonates
    CALCITE
    DOLOMITE
    SIDERITE
"Clays"
    CHLORITES
    HALLOYSITE
    ILLITES
      2M
      1M
    ILLITE/SMECTITE
    KAOLINITE
      disordered
      ordered
    SEPIOLITE
    PYROPHYLLITE
    SMECTITE

Iron Minerals
    GOETHITE
    HEMATITE
Micas
    MUSCOVITE
Sulfates
    GYPSUM
    JAROSITE
    ALUNITE
Others
    BUDDINGTONITE
    TALC
Vegetation
    GREEN
    DRY

Spectral database work over the course of this research consisted primarily of collection and measurement of samples using the laboratory spectrometer and preparation of the initial volume of the spectral database for publication. Only the analytical work important to development of the expert system was supported by

this grant. Additional support was provided by CSES internal funds and IGCP-264. Spectra were measured at high resolution (constant 3.8 nm) and analyzed using the automated feature extraction procedures described above. Detailed X-Ray Diffraction (XRD) analyses and energy dispersive X-Ray (EDX) measurements were made. Additional high-quality Scanning Electron Microscope photographs were acquired. The digital reflectance spectra and supporting basic analysis software were released during 1991 as part of SIPS (Kruse et al., 1993b). The hardcopy database is presently in press (Kruse and Hauff, 1993). It consists of 26 <u>well characterized</u> minerals of primary geologic importance collected as part of this research. A section on spectral variability shows numerous spectra exhibiting natural variation for selected mineral groups. Additional material was contributed by international participants of the IUGS sponsored IGCP-264 project (Remote Sensing Spectral Properties) including sections on soils and vegetation. Table 3 shows the Table of Contents for the hardcopy database. Figures 6 through 9 demonstrate analyses for one mineral (kaolinite). The database will be published during 1993 through AGU as a special publication.

TABLE 3.   Table of Contents from the IGCP-264 Spectral Properties Database

CONTENTS

INTRODUCTION
ACKNOWLEDGMENTS

1.0   USER SURVEY SUMMARY

    1.1   INTRODUCTION
    1.2   QUESTIONNAIRE RESPONSE SUMMARY
    1.3   DETAILED QUESTIONNAIRE RESPONSES

2.0   CHARACTERIZED STANDARDS

    2.1   SUMMARY OF MINERAL SAMPLES
    2.2   ANALYTICAL PARAMETERS
    2.3   MINERAL SUMMARIES
    2.4   REFERENCES

3.0   SELECTED CONTRIBUTED SPECTRA

    3.1   INTRODUCTION

    3.2   ROCKS AND MINERALS
        3.2.1   MINERAL VARIABILITY
        3.2.2   GRAIN SIZE EFFECTS

    3.3   SOILS.
        3.3.1   CANADIAN SOILS
        3.3.2   CHINESE SOILS

    3.4   VEGETATION
        3.4.1   GENERAL CHARACTERISTICS
        3.4.2   CANADIAN BOREAL FOREST VEGETATION,

4.0   SPECTRAL PROPERTIES - SELECTED BIBLIOGRAPHY.

Figure 6. Mineral summary sheet from the IGCP-264 spectral database for Kaolinite.

KAOLINITE

(including kaolinite and halloysite)

PROPERTIES

FORMULA: $Al_2Si_2O_5(OH)_4$
CRYSTAL SYSTEM: Triclinic *CLEAVAGE:* {001} perfect
HARDNESS: 2.0-2.5 *DENSITY:* 2.6-2.63
COLOR-LUSTER: Colorless, white, can be tinted yellowish, brownish, reddish or bluish. Transparent to translucent; pearly to dull earthy.
HABIT: Thin, hexagonal platelets or scales up to 2mm in size, many times stacked in books; as elongated plates or curved laths; usually massive, compact, friable or mealy; twinning rare.

OCCURRENCE

A very common clay mineral formed by weathering or hydrothermal alteration of feldspars and other aluminous silicate minerals in soils, permeable bedrock and warm, moist regions; as a diagenetic mineral filling pore spaces in sedimentary rocks, and massive lacustrine, lagoonal or deltaic, kaolin deposits. It is a common associate of hot springs hydrothermal ore deposits, and acid sulfate volcanic hosted ore deposits. It is also found as an "underclay" in coal deposits.

SIMILAR SPECIES:

Dickite, Nacrite, Halloysite

ASSOCIATED SPECIES:

Feldspar, quartz, alunite, silica, other clay minerals, iron oxides, pyrite, siderite, anatase, rutile

REFERENCES:

Brindley, G.W., and Brown, G., 1980, *Crystal Structures of Clay Minerals and Their X-ray Diffraction:* Mineralogical Society Monograph No. 5, Mineralogical Society, London, 495 pages.
Deer, W.A., Howie, R.A., and Zussman, J., 1962, *The Rock Forming Minerals*, 3, 194-212, New York, Wiley.
Newman, A.C.D., 1987, *Chemistry of Clays and Clay Minerals:* Mineralogical Society Monograph No. 6, Mineralogical Society, London, Great Britain, 480 p.

SOURCE

Washington County, Georgia, **CSES-KL500**, [CMS-KGa-1], Clay Minerals Society Source Clay KGa-1, *well crystalline kaolinite*
Cripple Creek Hydrothermal Ore deposit, **CSES-KL502**, Dan Taranik, University of Colorado, Masters Thesis, *poorly crystalline kaolinite.*

Figure 7.

Figure 7. Reflectance spectra from the IGCP-264 spectral database for kaolinite. The file extensions refer to the spectrometer; .sir=SIRIS, .rlb=Relab, .cse=CSES beckman, .usg=USGS beckman, .pm2=PIMA.

STACKED REFLECTANCE SPECTRA OF KAOLINITE KL500 (WELL CRYSTALLINE)
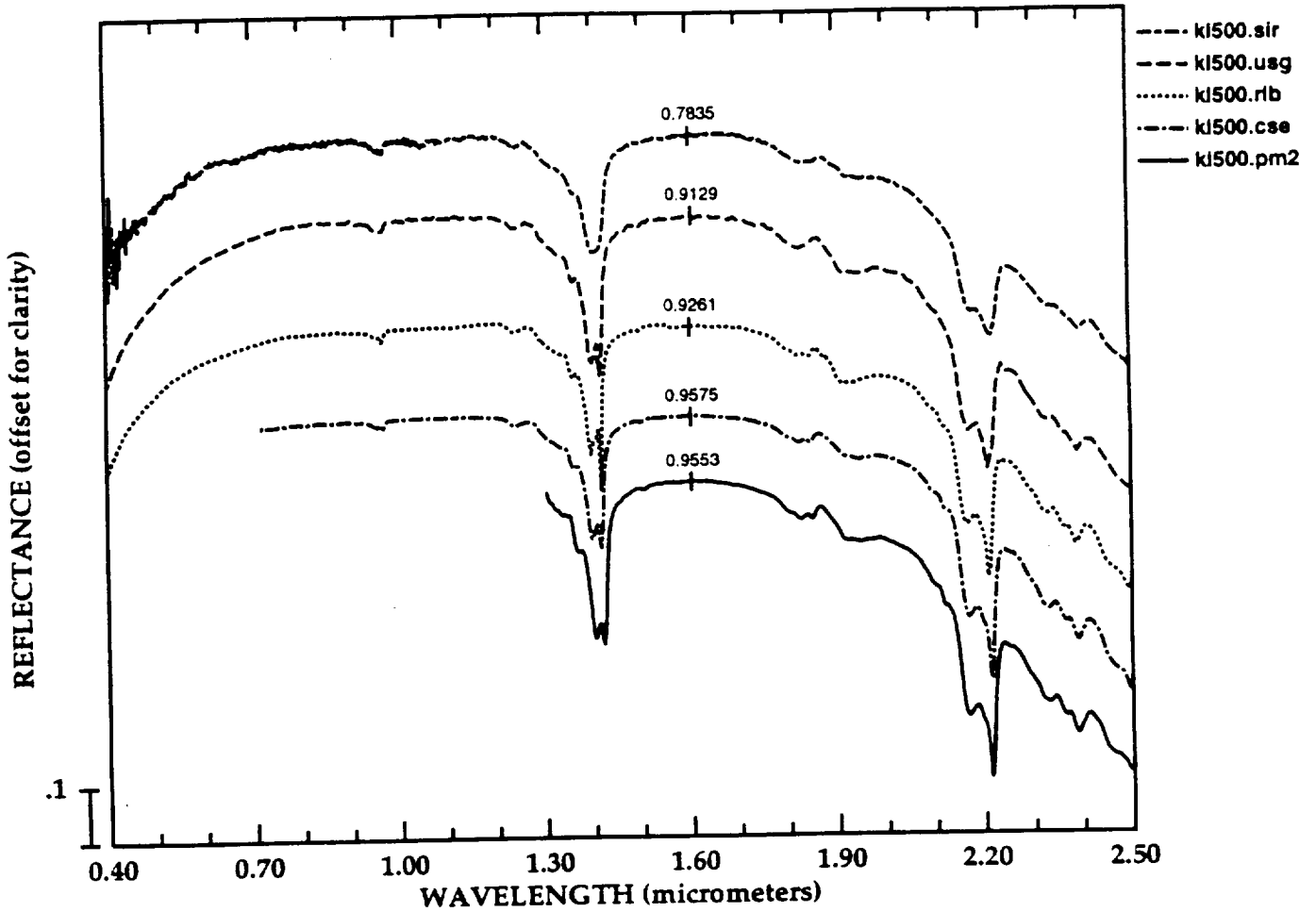
ABSORPTION BAND ANALYSIS FOR KAOLINITE KL500

Spectra Filename: kl500.rlb   Data Filename: kl500.bnd

band	order	wave	depth	FWHM	asym
1	1/ 2	2.2050	0.3317	0.0665	-0.6491
	2/ 2	2.1600	0.2330	0.0740	0.3997
2	1/ 2	1.4150	0.3254	0.0352	-0.6249
	2/ 2	1.3950	0.2574	0.0424	-0.0887
3	1/ 2	2.3800	0.0747	0.0239	-0.2004
	2/ 2	2.3550	0.0407	0.0493	0.7834
4	1/ 2	2.4850	0.0555	0.0805	-0.2052
	2/ 2	2.4450	0.0503	0.0830	0.7004
5	1/ 1	1.9100	0.0467	0.0530	0.3200
6	1/ 1	2.3150	0.0397	0.0300	-0.2576
7	1/ 1	1.8150	0.0271	0.0644	-0.0602
8	1/ 2	0.9650	0.0239	0.0228	-0.6107
	2/ 2	0.9550	0.0163	0.0308	-0.0941

Figure 8. XRD analysis from the IGCP-264 spectral database for kaolinite

X-RAY DIFFRACTION ANALYSIS FOR KAOLINITE KL500
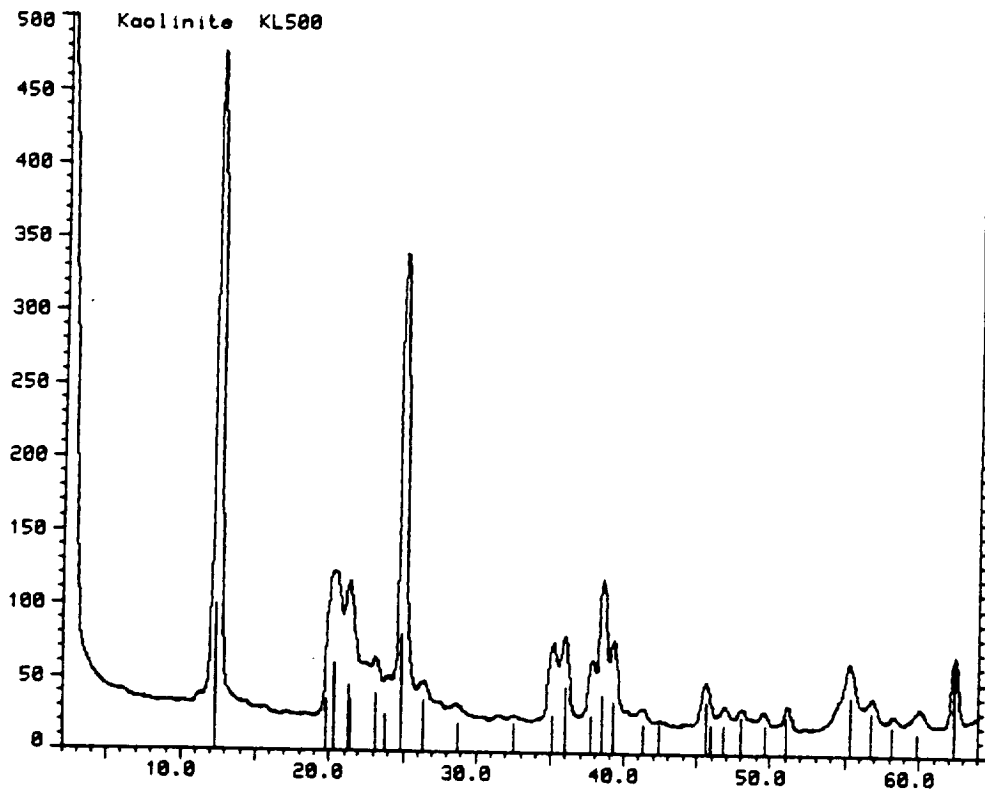
KAOLINITE *JCPDS # 14-164*

	dÅ	INT.	2THETA	h k l		dÅ	INT.	2THETA	h k l
1	7.170	100	12.335	0 0 1	16	2.293	35	39.258	1 3 1
2	4.478	35	19.810	0 2 0	17	2.186	20	41.265	2 0 1
3	4.366	60	20.323	1 -1 0	18	2.133	20	42.339	0 2 -3
4	4.186	45	21.207	1 1 -1	19	1.987	35	45.618	0 0 0
5	4.139	35	21.451	1 -1 -1	20	1.974	20	45.936	2 -2 1
6	3.847	40	23.101	0 2 -1	21	1.939	20	46.814	1 3 2
7	3.745	25	23.739	0 2 1	22	1.897	25	47.914	1 3 -3
8	3.579	80	24.857	0 0 2	23	1.838	20	49.554	2 0 2
9	3.376	35	26.378	1 1 1	24	1.789	25	51.007	0 0 4
10	3.107	20	28.709	1 -1 -2	25	1.660	40	55.294	1 -3 3
11	2.754	20	32.484	0 2 2	26	1.620	30	56.782	1 -5 1
12	2.553	25	35.121	1 3 0	27	1.586	20	58.113	1 3 -4
13	2.495	45	35.965	1 -3 1	28	1.545	15	59.810	1 -3 -4
14	2.385	25	37.685	0 0 3	29	1.489	60	62.305	3 3 -1
15	2.338	40	38.472	1 -3 1					

Figure 9.   Scanning electron micrograph and energy dispersive spectra of kaolinite from the IGCP-264 spectral database.

KAOLINITE

COUNTS

ENERGY keV

30kv 036
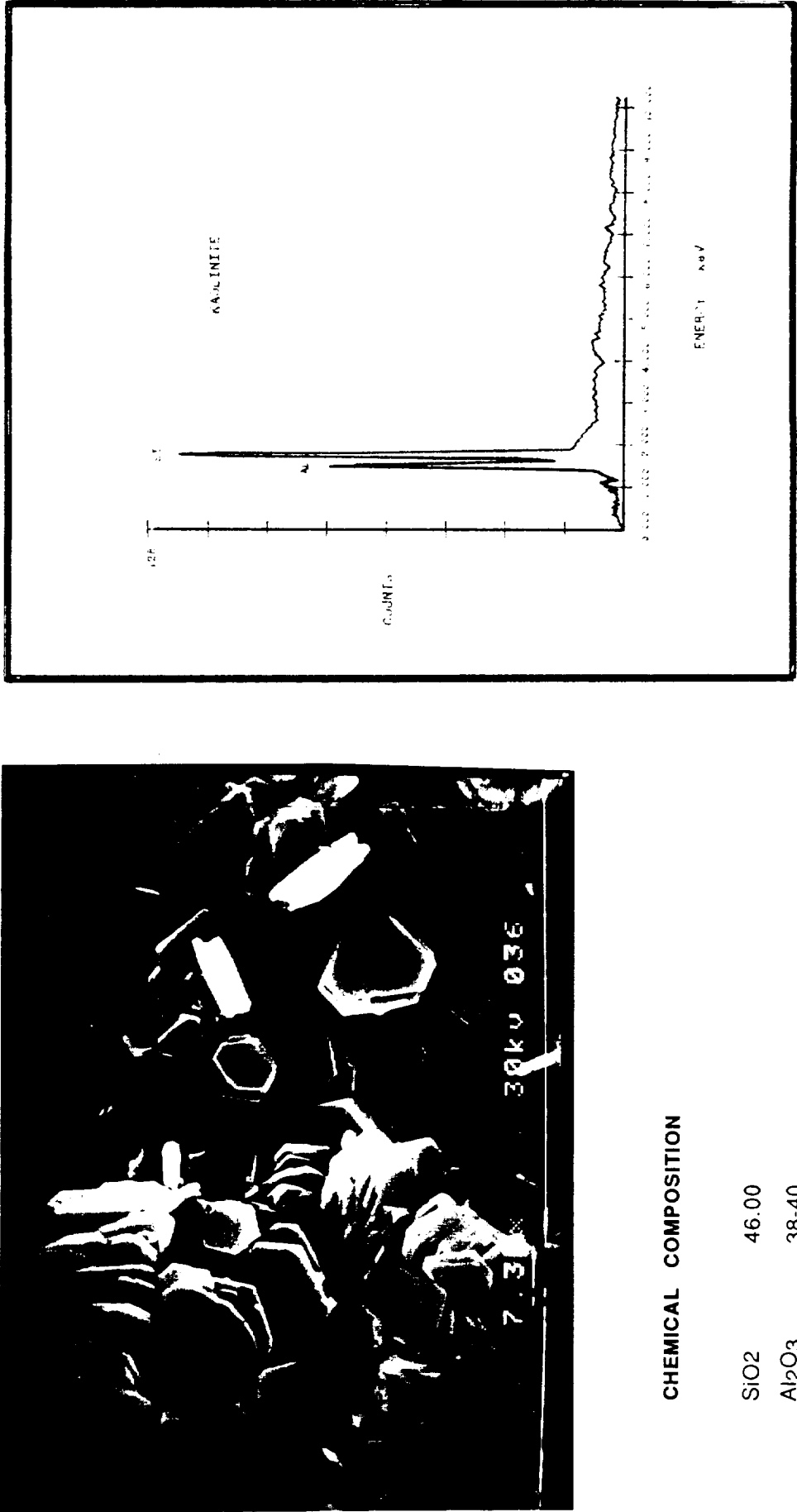
CHEMICAL COMPOSITION

SiO2   46.00
Al2O3   38-40
H2O   14.00

REF: Deer et al, 1962

MINERAL SPECTRAL FEATURES

Spectra measured for the IGCP-264 spectral database were analyzed using the feature extraction software to build fact tables containing all of the spectral features found for each mineral as discussed previously and shown in Table 1. These features were interactively analyzed using the SFW program to build rules. The rules consist of features and attributes selected by the analyst (the PI in this case) as being representative for a specific material (Table 4). In addition, each feature was assigned a weight from 0 (not required for identification) to 1.0 (mandatory for identification) corresponding to its importance. The rules shown in Table 4 list all of the selected features for the default expert system rule-base. These represent a minimum set of rules for mineralogical mapping in geologic applications. They are easily updated or modified as additional spectra or spectral statistics become available.

MINERAL VARIATION - GEOLOGIC MAPPING IMPLICATIONS
MIXED LAYER KAOLINITE/SMECTITE EXAMPLE

One of the major problems and most exciting areas of research in analysis of mineral spectra is in the area of mineral variation. Most past studies have tried to measure one characteristic spectrum for a particular mineral. While this provides a starting point, it is actually an unrealistic simplification, as minerals exhibit a large amount of natural variability. This research has taken the first steps towards quantitative characterization of mineral variability. We have begun to develop mathematical models that can explain the spectral characteristics in terms of the chemical and structural make up of the minerals.

Figure 10 shows pure kaolinite and smectite endmember spectra and selected spectra of a suite of mixed layer kaolinite/smectite clays from the Argiles Plastiques Formation, Paris Basin, France. Note the regular variation of the 2.2 μm absorption feature. The proportion of the kaolinite and smectite layers were determined from X-ray diffraction (XRD) peak migration curves calculated by Reynolds (1980) and Brindley et al. (1983). This sequence is important because it records the conditions of deposition and subsequent weathering environment of the basin (Thiry, 1989). The mixed layer kaolinite/smectites generally occur in continental sedimentary deposits developed on shales, chalk, and limestones. They often appear in the soil profile from smectite adjacent to bedrock to kaolinite in the near-surface environment. Recognition of the interstratified minerals can be very important to characterizing bedrock composition, soil genesis, and paleoclimate (Shimoyama et al, 1969; Wiewiora, A., 1971; Schultz et al., 1971; Wilson and Gradwick, 1972; Lucas et al., 1974; Yerima et al, 1985).

Although the sequence shown in Figure 10 has been recognized through XRD studies and field investigations, the XRD recognition and quantification is difficult and extensive studies have not been conducted. Analysis of laboratory reflectance spectra, and particularly of in-situ materials using a field spectrometer has produced new insights to the occurrence and distribution of these minerals. An experienced analyst can see immediately from Figure 10 that there is a progression in the shapes of the spectral features from the pure kaolinite endmember to the smectite endmember. The continuum removal and feature extraction procedures described

RULE_FILE
LIB=igcp_264_usgs.slb

Table 4. Default rules from SFW.

ACTINOLITE_am3000 #Features 4

Weight	Position	Tolerance	Binary encoding Parameters 2.00000 2.40000 Depth	Tolerance	FWHM	Tolerance	Asymm	Tolerance
0.30000	1.03800	0.02000	0.57053	0.00000	0.55449	0.02000	-0.26907	0.00000
1.00000	2.31500	0.02000	0.44800	0.00000	0.04859	0.02000	-0.31199	0.00000
0.30000	1.39300	0.02000	0.31580	0.00000	0.01275	0.02000	0.51121	0.00000
1.00000	2.38600	0.02000	0.25604	0.00000	0.03017	0.02000	0.14740	0.00000

ALUNITE_K_al705 #Features 4

Weight	Position	Tolerance	Binary encoding Parameters 2.00000 2.40000 Depth	Tolerance	FWHM	Tolerance	Asymm	Tolerance
1.00000	2.16500	0.02000	0.37318	0.00000	0.10219	0.02000	-0.10095	0.00000
0.20000	2.21500	0.02000	0.26392	0.00000	0.11628	0.02000	-1.16594	0.00000
1.00000	2.32500	0.02000	0.16622	0.00000	0.03024	0.02000	-0.18854	0.00000
0.60000	1.76400	0.02000	0.12116	0.00000	0.04991	0.02000	-0.14785	0.00000

ALUNITE_Na_al706 #Features 4

Weight	Position	Tolerance	Binary encoding Parameters 2.00000 2.40000 Depth	Tolerance	FWHM	Tolerance	Asymm	Tolerance
1.00000	2.17500	0.02000	0.35612	0.00000	0.09881	0.02000	-0.21739	0.00000
0.20000	2.21500	0.02000	0.23707	0.00000	0.13305	0.02000	-0.91083	0.00000
1.00000	2.32500	0.02000	0.17091	0.00000	0.03303	0.02000	0.01244	0.00000
0.60000	1.76400	0.02000	0.14757	0.00000	0.05292	0.02000	-0.15998	0.00000

BUDDINGTONITE_nhb2301 #Features 3

Weight	Position	Tolerance	Binary encoding Parameters 2.00000 2.40000 Depth	Tolerance	FWHM	Tolerance	Asymm	Tolerance
1.00000	2.12500	0.02000	0.25769	0.00000	0.22012	0.02000	0.04708	0.00000
1.00000	2.01500	0.02000	0.14873	0.00000	0.27505	0.02000	1.07181	0.00000
0.60000	1.90500	0.02000	0.02284	0.00000	0.02600	0.02000	-0.16291	0.00000

20

Table 4. Default rules from SFW.(continued)

CALCITE_co2004

#Features	Binary encoding Parameters	
4	2.00000	2.40000

Weight	Position	Tolerance	Depth	Tolerance	FWHM	Tolerance	Asymm	Tolerance
1.00000	2.33500	0.02000	0.27390	0.00000	0.08649	0.02000	-0.31800	0.00000
0.30000	1.99500	0.02000	0.08131	0.00000	0.17061	0.02000	-0.63415	0.00000
0.30000	1.87500	0.02000	0.07949	0.00000	0.17202	0.02000	0.52166	0.00000
0.20000	2.15500	0.02000	0.03134	0.00000	0.03294	0.02000	-0.12079	0.00000

CHLORITE_ch2402

#Features	Binary encoding Parameters	
2	2.00000	2.40000

Weight	Position	Tolerance	Depth	Tolerance	FWHM	Tolerance	Asymm	Tolerance
1.00000	2.32500	0.02000	0.28062	0.00000	0.13285	0.02000	-0.21497	0.00000
1.00000	2.25500	0.02000	0.22345	0.00000	0.14277	0.02000	0.68753	0.00000

DOLOMITE_cod2005

#Features	Binary encoding Parameters	
4	2.00000	2.40000

Weight	Position	Tolerance	Depth	Tolerance	FWHM	Tolerance	Asymm	Tolerance
1.00000	2.31500	0.02000	0.21709	0.00000	0.09172	0.02000	-0.31849	0.00000
0.30000	1.98500	0.02000	0.04671	0.00000	0.10639	0.02000	-0.68919	0.00000
0.30000	1.86500	0.02000	0.03339	0.00000	0.04873	0.02000	0.61234	0.00000
0.20000	2.13500	0.02000	0.01091	0.00000	0.02546	0.02000	0.28675	0.00000

DRY_VEG_siris

#Features	Binary encoding Parameters	
5	0.401000	2.40000

Weight	Position	Tolerance	Depth	Tolerance	FWHM	Tolerance	Asymm	Tolerance
0.20000	1.92500	0.02000	0.36840	0.00000	0.07557	0.02000	0.21467	0.00000
0.20000	1.46900	0.02000	0.29502	0.00000	0.16998	0.02000	0.11723	0.00000
1.00000	2.09500	0.02000	0.17001	0.00000	0.09860	0.02000	0.13648	0.00000
0.30000	1.72400	0.02000	0.09341	0.00000	0.11558	0.02000	0.40806	0.00000
1.00000	2.31000	0.02000	0.07215	0.00000	0.02994	0.02000	-0.20220	0.00000

Table 4. Default rules from SFW.(continued)

GOETHITE_fe2600

#Features 3   Binary encoding Parameters   0.401000   1.20000

Weight	Position	Tolerance	Depth	Tolerance	FWHM	Tolerance	Asymm	Tolerance
1.00000	0.93000	0.03000	0.36083	0.00000	0.28127	0.02000	0.23955	0.00000
0.80000	0.48000	0.02000	0.30411	0.00000	0.04588	0.02000	0.07175	0.00000
0.30000	0.66800	0.02000	0.13251	0.00000	0.08714	0.02000	0.03544	0.00000

GREEN_VEG_elvidge

#Features 6   Binary encoding Parameters   0.401000   2.40000

Weight	Position	Tolerance	Depth	Tolerance	FWHM	Tolerance	Asymm	Tolerance
0.40000	1.43900	0.02000	0.73335	0.00000	0.19096	0.02000	0.08483	0.00000
0.20000	1.20000	0.02000	0.20952	0.00000	0.09636	0.02000	1.39724	0.00000
0.20000	0.98500	0.02000	0.20821	0.00000	0.09667	0.02000	1.20187	0.00000
1.00000	0.68200	0.02000	0.69672	0.00000	0.11715	0.02000	-0.41653	0.00000
0.40000	1.92500	0.02000	0.69236	0.00000	0.21897	0.02000	0.51511	0.00000
0.20000	1.76000	0.02000	0.16052	0.00000	0.19932	0.02000	0.62194	0.00000

GYPSUM_su2202

#Features 5   Binary encoding Parameters   2.00000   2.40000

Weight	Position	Tolerance	Depth	Tolerance	FWHM	Tolerance	Asymm	Tolerance
0.40000	1.53400	0.02000	0.22525	0.00000	0.18187	0.02000	-0.49223	0.00000
1.00000	2.21500	0.02000	0.16990	0.00000	0.09967	0.02000	-0.12449	0.00000
0.60000	2.17500	0.02000	0.12560	0.00000	0.14492	0.02000	0.41597	0.00000
0.60000	2.26500	0.02000	0.09947	0.00000	0.16534	0.02000	-0.84471	0.00000
0.60000	1.74800	0.02000	0.16909	0.00000	0.06793	0.02000	0.17952	0.00000

HALLOYSITE_klh503

#Features 6   Binary encoding Parameters   2.00000   2.40000

Weight	Position	Tolerance	Depth	Tolerance	FWHM	Tolerance	Asymm	Tolerance
0.20000	1.41300	0.02000	0.51465	0.00000	0.07410	0.02000	0.04401	0.00000
0.20000	1.38800	0.02000	0.45672	0.00000	0.09177	0.02000	0.40818	0.00000
1.00000	2.20500	0.02000	0.41611	0.00000	0.06041	0.02000	-0.33263	0.00000
0.20000	1.91500	0.02000	0.39715	0.00000	0.09493	0.02000	0.41967	0.00000
0.30000	2.38600	0.02000	0.06508	0.00000	0.11280	0.02000	-0.22116	0.00000
0.20000	2.31500	0.02000	0.06495	0.00000	0.11287	0.02000	0.78585	0.00000

Table 4. Default rules from SFW.(continued)

HEMATITE_fe2602

#Features 2

Binary encoding Parameters 0.401000   1.20000

Weight	Position	Tolerance	Depth	Tolerance	FWHM	Tolerance	Asymm	Tolerance
1.00000	0.86900	0.03000	0.47050	0.00000	0.21124	0.02000	0.27626	0.00000
0.80000	0.55100	0.05000	0.03333	0.00000	0.02188	0.02000	1.28362	0.00000

ILLITE_1M_il105

#Features 5

Binary encoding Parameters 2.00000   2.40000

Weight	Position	Tolerance	Depth	Tolerance	FWHM	Tolerance	Asymm	Tolerance
0.30000	1.90500	0.02000	0.11051	0.00000	0.08147	0.02000	-0.61147	0.00000
1.00000	2.20500	0.02000	0.07292	0.00000	0.06058	0.02000	0.24394	0.00000
0.30000	1.41300	0.02000	0.04640	0.00000	0.02964	0.02000	0.14260	0.00000
0.40000	2.35500	0.02000	0.02728	0.00000	0.04715	0.02000	-0.30744	0.00000
0.40000	2.45000	0.02000	0.01004	0.00000	0.01229	0.02000	1.41490	0.00000

ILLITE_2M_il101

#Features 5

Binary encoding Parameters 2.00000   2.40000

Weight	Position	Tolerance	Depth	Tolerance	FWHM	Tolerance	Asymm	Tolerance
1.00000	2.19500	0.02000	0.34252	0.00000	0.04900	0.02000	0.12634	0.00000
0.30000	1.40800	0.02000	0.29035	0.00000	0.02955	0.02000	0.21463	0.00000
0.30000	1.91500	0.02000	0.15713	0.00000	0.07813	0.02000	0.32225	0.00000
0.60000	2.34500	0.02000	0.11683	0.00000	0.04715	0.02000	-0.20096	0.00000
0.60000	2.44000	0.02000	0.09641	0.00000	0.05750	0.02000	-0.05674	0.00000

IS_RECTORITE_isr202

#Features 6

Binary encoding Parameters 2.00000   2.40000

Weight	Position	Tolerance	Depth	Tolerance	FWHM	Tolerance	Asymm	Tolerance
0.30000	1.91500	0.02000	0.27919	0.00000	0.11166	0.02000	0.47061	0.00000
0.30000	1.40800	0.02000	0.22398	0.00000	0.03663	0.02000	0.46443	0.00000
0.30000	1.46400	0.02000	0.08851	0.00000	0.11994	0.02000	-0.40382	0.00000
1.00000	2.18500	0.02000	0.14612	0.00000	0.05537	0.02000	0.10089	0.00000
0.30000	2.43000	0.02000	0.14000	0.00000	0.06381	0.02000	0.29921	0.00000
0.30000	2.32500	0.02000	0.03470	0.00000	0.05327	0.02000	0.30000	0.00000

Table 4.   Default rules from SFW.(continued)

JAROSITE_jr2501

#Features: 7

Binary encoding Parameters: 2.00000   2.40000

Weight	Position	Tolerance	Depth	Tolerance	FWHM	Tolerance	Asymm	Tolerance
0.20000	0.43700	0.02000	0.42339	0.00000	0.02480	0.02000	0.46981	0.00000
1.00000	0.93000	0.03000	0.33702	0.00000	0.33314	0.02000	0.19541	0.00000
1.00000	2.26500	0.02000	0.23890	0.00000	0.05325	0.02000	-0.28319	0.00000
1.00000	2.21500	0.02000	0.12870	0.00000	0.12950	0.02000	0.42071	0.00000
0.40000	1.46900	0.02000	0.10255	0.00000	0.06712	0.02000	0.48609	0.00000
0.40000	1.51300	0.02000	0.05595	0.00000	0.10663	0.02000	-0.22566	0.00000
0.60000	1.85500	0.02000	0.08611	0.00000	0.03428	0.02000	-0.20052	0.00000

KAOLINITE_P_XSTAL_kl502

#Features: 5

Binary encoding Parameters: 2.00000   2.40000

Weight	Position	Tolerance	Depth	Tolerance	FWHM	Tolerance	Asymm	Tolerance
1.00000	2.20500	0.02000	0.43205	0.00000	0.07103	0.02000	-0.36491	0.00000
0.80000	2.16500	0.02000	0.28542	0.00000	0.08045	0.02000	0.45323	0.00000
0.30000	1.41300	0.02000	0.34993	0.00000	0.04437	0.02000	-0.16448	0.00000
0.30000	1.39300	0.02000	0.31137	0.00000	0.04938	0.02000	0.24484	0.00000
0.30000	1.91500	0.02000	0.24424	0.00000	0.05789	0.02000	0.29967	0.00000

KAOLINITE_W_XSTAL_kl500

#Features: 7

Binary encoding Parameters: 2.00000   2.40000

Weight	Position	Tolerance	Depth	Tolerance	FWHM	Tolerance	Asymm	Tolerance
1.00000	2.20500	0.02000	0.32452	0.00000	0.07185	0.02000	-0.54577	0.00000
1.00000	2.16500	0.02000	0.25838	0.00000	0.07711	0.02000	0.33188	0.00000
0.30000	1.41300	0.02000	0.31686	0.00000	0.04395	0.02000	-0.44953	0.00000
0.30000	1.39800	0.02000	0.29228	0.00000	0.04664	0.02000	-0.11524	0.00000
0.60000	2.38600	0.02000	0.05952	0.00000	0.02403	0.02000	-0.51408	0.00000
0.30000	1.91500	0.02000	0.04801	0.00000	0.05605	0.02000	0.11757	0.00000
0.60000	2.31500	0.02000	0.04327	0.00000	0.04390	0.02000	-0.35566	0.00000

Table 4. Default rules from SFW.(continued)

MUSCOVITE_il107

#Features 5
Binary encoding Parameters 2.00000 2.40000

Weight	Position	Tolerance	Depth	Tolerance	FWHM	Tolerance	Asymm	Tolerance
1.00000	2.21500	0.02000	0.21147	0.00000	0.05892	0.02000	0.04332	0.00000
0.30000	1.41300	0.02000	0.14250	0.00000	0.02950	0.02000	0.11917	0.00000
0.30000	1.92500	0.02000	0.05675	0.00000	0.08595	0.02000	0.28761	0.00000
0.60000	2.34500	0.02000	0.05656	0.00000	0.03661	0.02000	-0.00657	0.00000
0.40000	2.44000	0.02000	0.03643	0.00000	0.05541	0.02000	0.24662	0.00000

NONTRONITE_smn454

#Features 4
Binary encoding Parameters 2.00000 2.40000

Weight	Position	Tolerance	Depth	Tolerance	FWHM	Tolerance	Asymm	Tolerance
0.60000	1.90500	0.02000	0.73469	0.00000	0.14495	0.02000	0.53161	0.00000
0.60000	1.41300	0.02000	0.61270	0.00000	0.12312	0.02000	0.42424	0.00000
0.60000	2.30000	0.02000	0.21801	0.00000	0.10000	0.02000	0.06048	0.00000
1.00000	2.20500	0.02000	0.18878	0.00000	0.05132	0.02000	0.15920	0.00000

PYROPHYLLITE_py602

#Features 5
Binary encoding Parameters 2.00000 2.40000

Weight	Position	Tolerance	Depth	Tolerance	FWHM	Tolerance	Asymm	Tolerance
0.30000	1.39300	0.02000	0.37736	0.00000	0.01181	0.02000	-0.14059	0.00000
1.00000	2.16500	0.02000	0.30650	0.00000	0.02798	0.02000	0.31136	0.00000
1.00000	2.31500	0.02000	0.22360	0.00000	0.03756	0.02000	-0.43997	0.00000
0.30000	1.94500	0.02000	0.16876	0.00000	0.07520	0.02000	0.02417	0.00000
0.30000	2.38600	0.02000	0.05218	0.00000	0.02709	0.02000	0.33634	0.00000

SEPIOLITE_sep3101

#Features 6
Binary encoding Parameters 2.00000 2.40000

| Weight	Position	Tolerance	Depth	Tolerance	FWHM	Tolerance	Asymm	Tolerance
0.60000	1.91500	0.02000	0.59081	0.00000	0.11251	0.02000	0.45474	0.00000
0.60000	1.41800	0.02000	0.30004	0.00000	0.12337	0.02000	0.41926	0.00000
0.30000	1.38800	0.02000	0.25122	0.00000	0.13729	0.02000	0.95397	0.00000
1.00000	2.31500	0.02000	0.14713	0.00000	0.03453	0.02000	-0.40537	0.00000
1.00000	2.38600	0.02000	0.09931	0.00000	0.04916	0.02000	0.40265	0.00000
0.20000	1.16300	0.02000	0.02979	0.00000	0.03772	0.02000	0.20112	0.00000

Table 4. Default rules from SFW.(continued)

SIDERITE_cos2002 #Features 4 Binary encoding Parameters 2.00000 2.40000

Weight	Position	Tolerance	Depth	Tolerance	FWHM	Tolerance	Asymm	Tolerance
0.60000	1.02000	0.02000	0.61668	0.00000	0.62617	0.02000	-0.10574	0.00000
0.60000	1.28000	0.02000	0.61457	0.00000	0.62692	0.02000	-0.13448	0.00000
1.00000	2.33000	0.02000	0.10535	0.00000	0.10513	0.02000	-0.36752	0.00000
0.30000	1.94500	0.02000	0.05615	0.00000	0.11674	0.02000	0.15503	0.00000

SMECTITE_Ca_smc403 #Features 3 Binary encoding Parameters 2.00000 2.40000

Weight	Position	Tolerance	Depth	Tolerance	FWHM	Tolerance	Asymm	Tolerance
0.80000	1.90500	0.02000	0.42369	0.00000	0.09582	0.02000	0.56305	0.00000
0.80000	1.41300	0.02000	0.24099	0.00000	0.08087	0.02000	0.39816	0.00000
1.00000	2.21500	0.02000	0.16187	0.00000	0.03799	0.02000	-0.17481	0.00000

SMECTITE_Na_smm402 #Features 3 Binary encoding Parameters 2.00000 2.40000

Weight	Position	Tolerance	Depth	Tolerance	FWHM	Tolerance	Asymm	Tolerance
0.80000	1.91500	0.02000	0.29384	0.00000	0.09733	0.02000	0.34893	0.00000
0.80000	1.41300	0.02000	0.20316	0.00000	0.04611	0.02000	0.25213	0.00000
1.00000	2.21500	0.02000	0.14978	0.00000	0.06256	0.02000	-0.07949	0.00000

TALC_tl2702 #Features 8 Binary encoding Parameters 2.00000 2.40000

Weight	Position	Tolerance	Depth	Tolerance	FWHM	Tolerance	Asymm	Tolerance
1.00000	2.31500	0.02000	0.46027	0.00000	0.04570	0.02000	-0.47646	0.00000
0.30000	1.39300	0.02000	0.36428	0.00000	0.01051	0.02000	0.31905	0.00000
1.00000	2.38600	0.02000	0.21630	0.00000	0.03181	0.02000	-0.00856	0.00000
0.30000	1.90500	0.02000	0.08959	0.00000	0.08054	0.02000	0.38888	0.00000
0.30000	2.00500	0.02000	0.03687	0.00000	0.15540	0.02000	-1.08264	0.00000
0.20000	2.07500	0.02000	0.06498	0.00000	0.03368	0.02000	0.87405	0.00000
0.20000	2.13500	0.02000	0.05204	0.00000	0.08466	0.02000	-0.25162	0.00000
0.20000	2.17500	0.02000	0.04099	0.00000	0.02732	0.02000	-0.95261	0.00000

Table 4.   Default rules from SFW.(continued)

#Features   Binary encoding Parameters
5   2.00000   2.40000

TREMOLITE_amt3001

Weight	Position	Tolerance	Depth	Tolerance	FWHM	Tolerance	Asymm	Tolerance
1.00000	2.31500	0.02000	0.43938	0.00000	0.04920	0.02000	-0.49760	0.00000
0.30000	1.39300	0.02000	0.42104	0.00000	0.00874	0.02000	-0.00659	0.00000
1.00000	2.38600	0.02000	0.26658	0.00000	0.02898	0.02000	-0.06133	0.00000
0.40000	1.03300	0.02000	0.21577	0.00000	0.16889	0.02000	-0.08055	0.00000
0.20000	2.11500	0.02000	0.07357	0.00000	0.02821	0.02000	0.33553	0.00000

27

Figure 10. Laboratory spectra of Paris Basin Kaolinite/Smectite Series. Note progression in shape from kaolinitic to smectitic for the 2.2, 1.9, and 1.4 μm absorption bands.
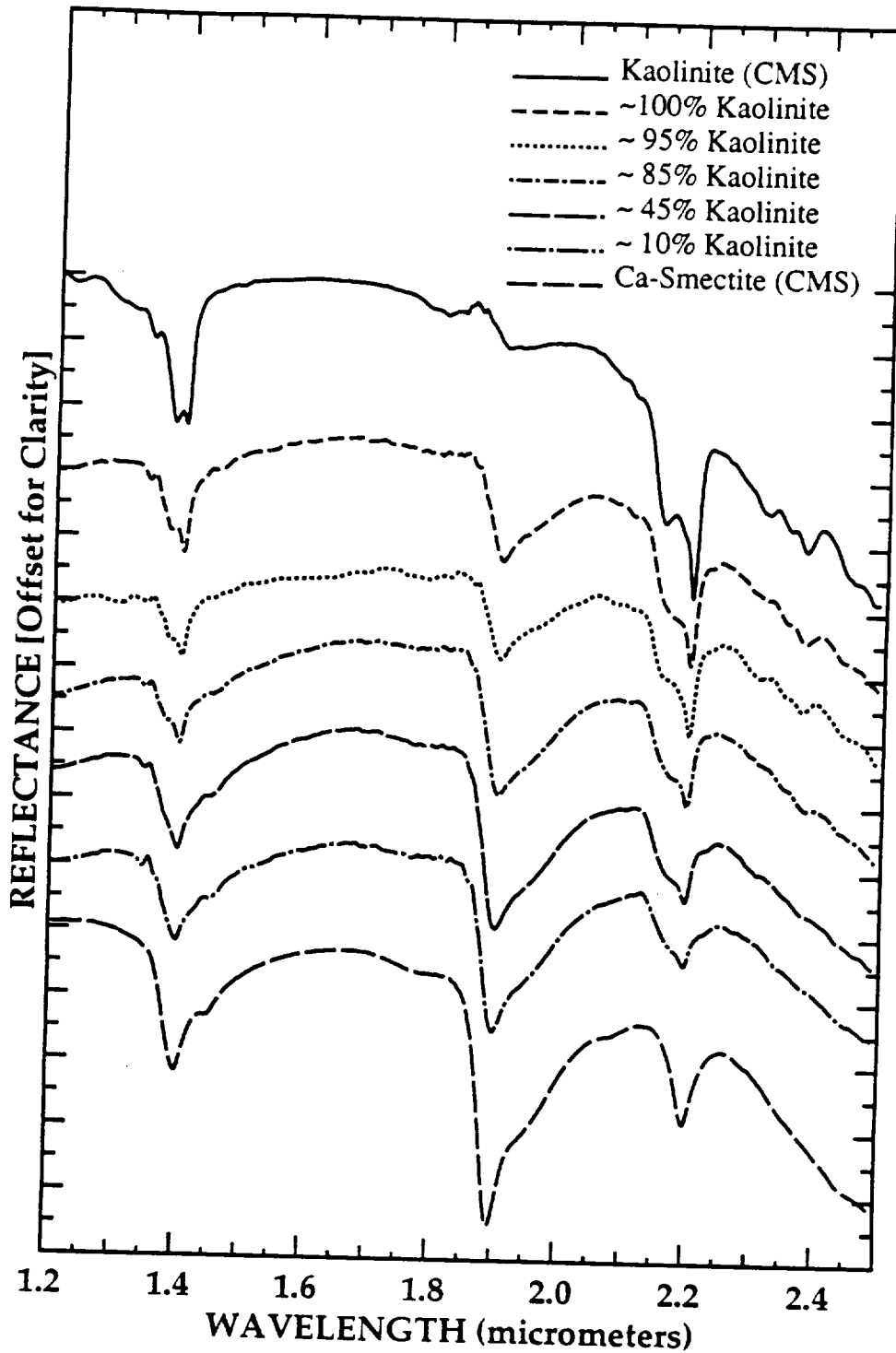
above provide a means of quantitatively characterizing this spectral progression. Similar variation can be seen in the 1.4 and 1.9 µm bands. Figure 11 is a plot of the asymmetry measurement for kaolinite/smectite samples from the Paris Basin, showing the relationship between the kaolinite content and the 2.2 µm band asymmetry. A linear regression to the data gives a correlation of $R^2=0.84$.

A field spectrometer was used during 1990 to measure, in-situ, naturally occurring kaolinite/smectite mixed layer clays (Kruse et al., 1991). Analyses of the 2.2 µm absorption features produced results comparable to those previously obtained in the laboratory with about 5-10% variation between field and laboratory measurements. This close correspondence is excellent, given the differences in illumination; surface effects such as grain-size, packing, and surface coatings; and atmospheric interference in field measurements. These measurements provide a rapid means of estimating kaolinite content for weathered rocks at their field location and have direct applicability to expert system design. These results confirm our ability to map mixed mineralogy (in this case the kaolinite component of mixed-layer kaolinite/smectite clays) using spectroscopic methods and open the potential for quantitative mapping using both field instruments and imaging spectrometer data.

VEGETATION VARIATION - ECOSYSTEM MAPPING IMPLICATIONS
GENERAL
Spectral properties of vegetation (Figure 12) are a function of leaf pigments (chlorophyll, xanthophyll, and carotene), cell morphology, internal refractive index discontinuities, water content, and other plant tissue constituents such as lignin, sugar, starch, and protein (Gates et al., 1965; Salisbury and Ross, 1969; Gates, 1970; Knipling, 1970; Thomas and Oerther, 1972. The pigments dominate the 0.30 to 0.70 µm region. A spectrum of green vegetation has major absorption features near 0.45 micrometers and 0.68 micrometers that can be attributed to chlorophyll. Healthy vegetation typically exhibits a sharp increase in reflectance near 0.70 micrometers and a plateau of high reflectance between about 0.70 and 1.30 µm. Minor water absorption features occurring near 0.96 and 1.20 µm have been related to both cellular arrangement and hydration state of the vegetation (Gates, 1970). Leaf water absorption dominates the region between 1.3 and 2.5 µm with healthy vegetation showing a general drop off in reflectance and strong molecular water bands at 1.4, and 1.9 µm. Plant tissue constituents also contribute to the overall spectrum.

Figure 13 and Table 5 show features extracted from green vegetation, and wet cotton cellulose. The green vegetation features closely match the wet cellulose features with the exception of the visible portion of the spectrum region where chlorophyll and other pigments dominate. The feature extraction and characterization software provides a quantitative means of analysis of the vegetation. Figure 14 and Table 5 show features extracted from the dry vegetation, and cotton cellulose. The dry vegetation features closely match the cellulose features. These results indicate that we should be able to develop rules through analysis of spectra with the feature extraction procedures to quantitatively map progressive changes from the wet (vigorous) to the dry (stressed) state.

Studies of plant constituents have also demonstrated that the SWIR (~1.0 - 2.5 µm) reflectance measurements can be used to obtain quantitative information about

29

Figure 11   Correlation of 2.2 μm absorption band asymmetry and percent
             kaolinite (determined by XRD) in mixed-layer kaolinite/smectite clays
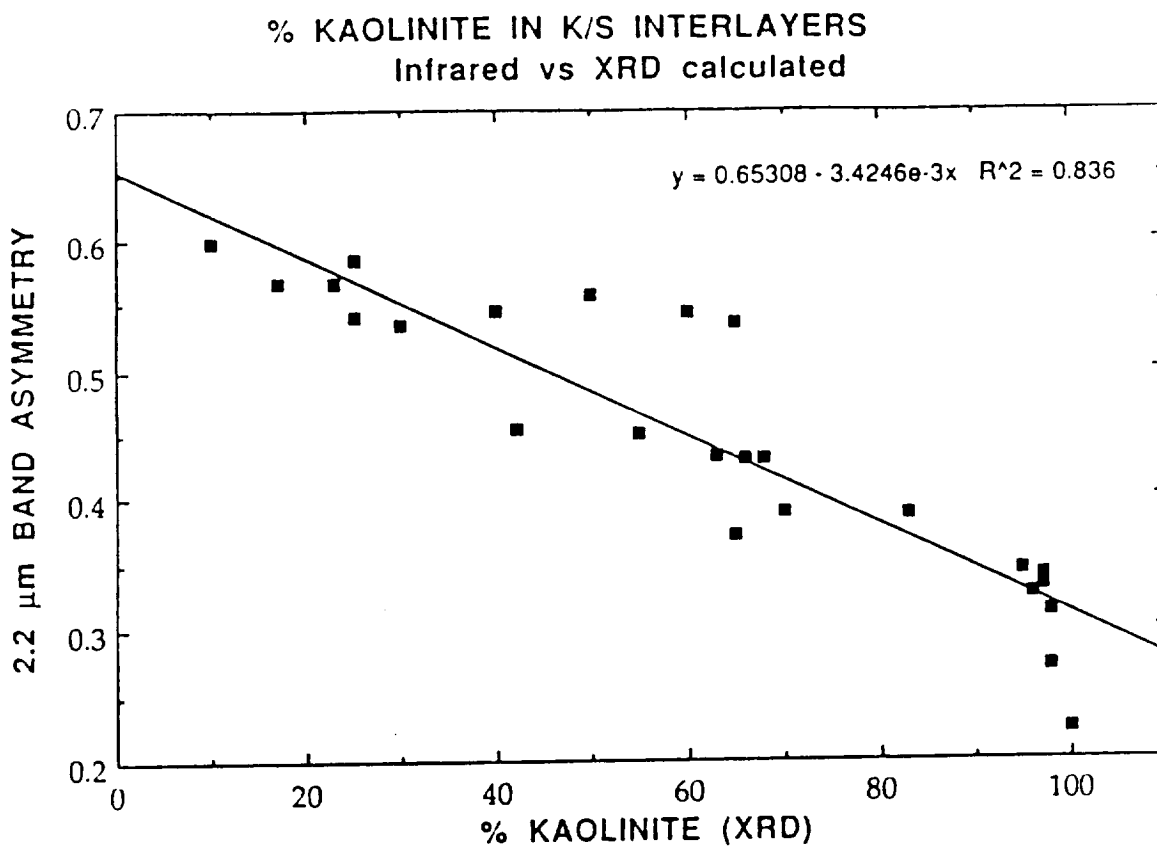   (From Hauff et al., 1990)

% KAOLINITE IN K/S INTERLAYERS
Infrared vs XRD calculated

$y = 0.65308 - 3.4246e\text{-}3x$ $R^2 = 0.836$

2.2 μm BAND ASYMMETRY

% KAOLINITE (XRD)

Figure 12. Typical reflectance spectrum of green vegetation in the visible, near-infrared, and short-wave infrared (From Ustin and Curtiss, 1989).
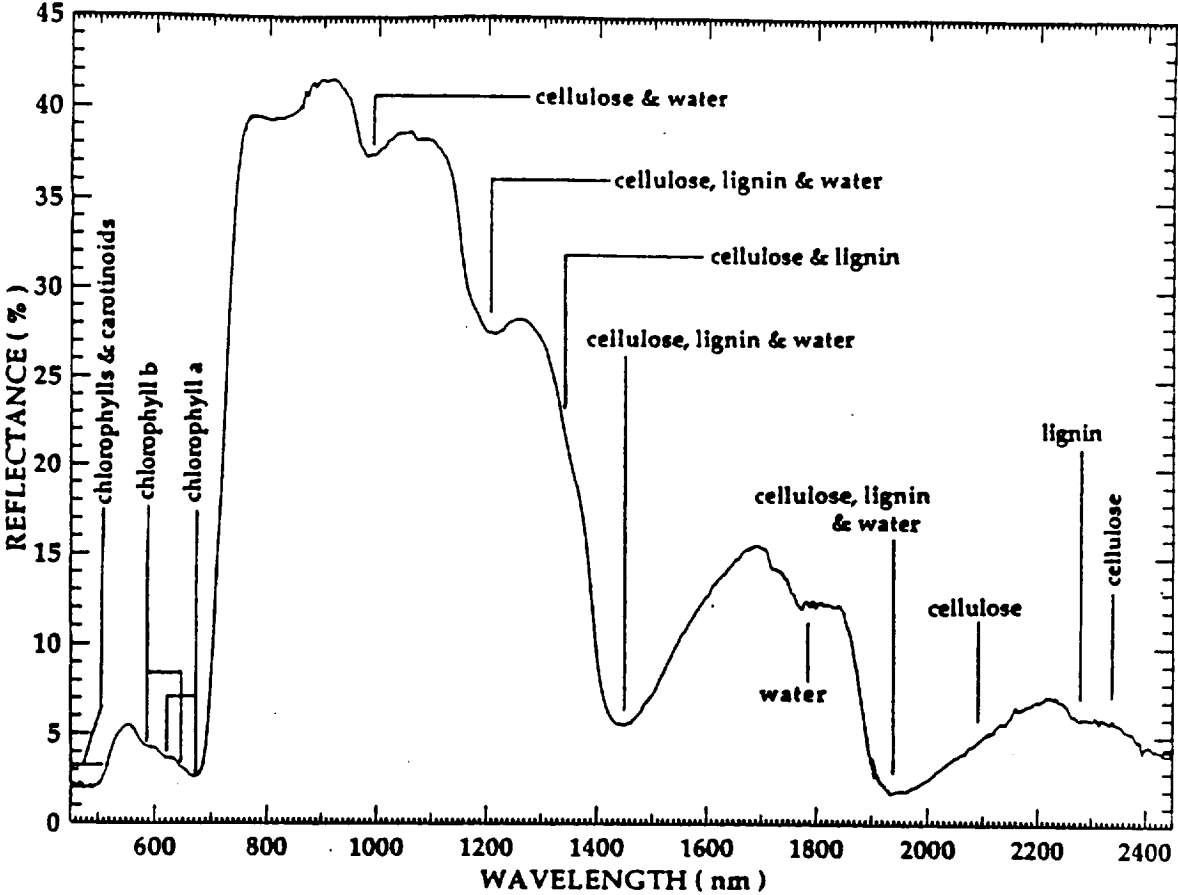
31

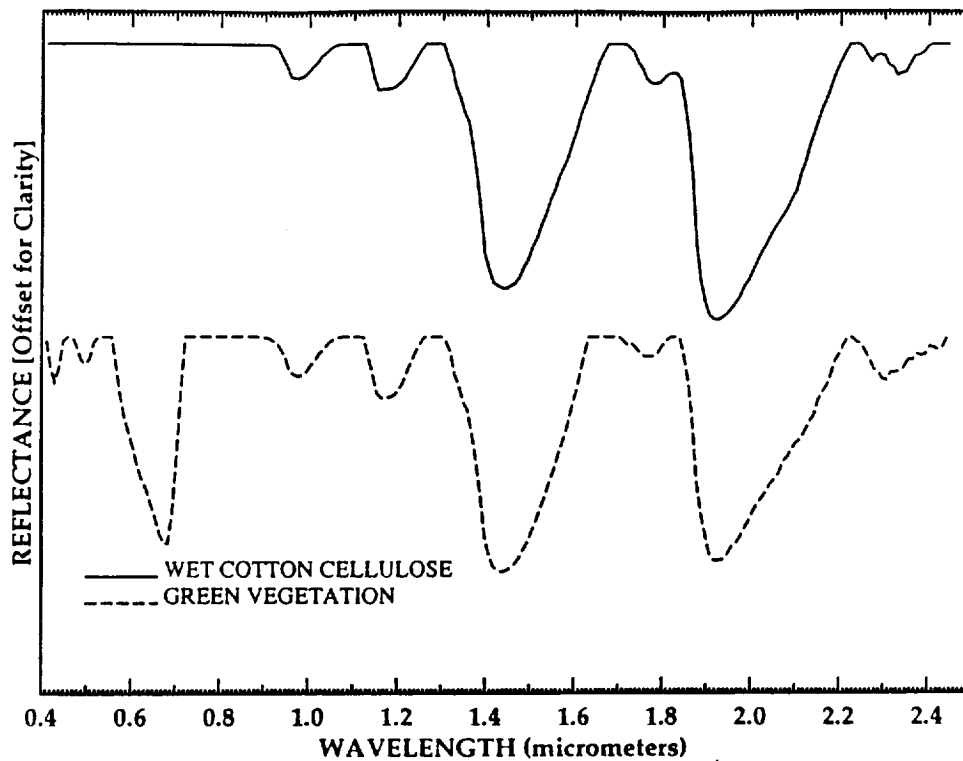Figure 13. Continuum-removed spectra of wet cotton cellulose and green vegetation.

Figure 14. Continuum-removed spectra of dry cotton cellulose and dry vegetation.
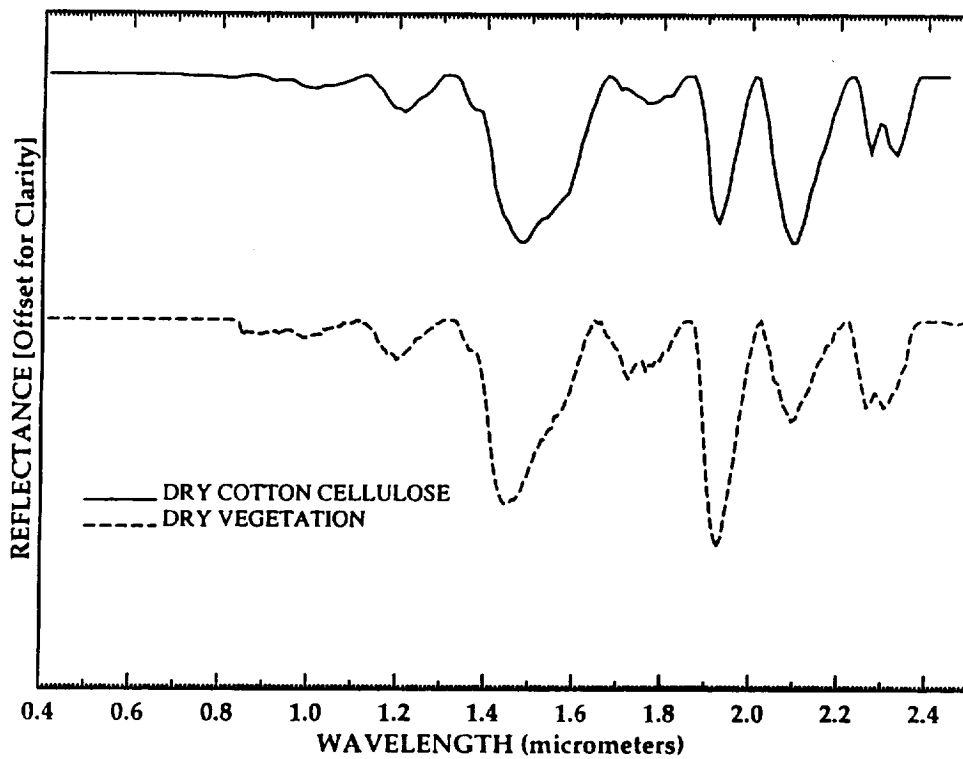
TABLE 5. COMPARISON OF GREEN AND DRY VEGETATION SPECTRAL FEATURES

SPECTRUM	B 1	B 2	B 3	BAND 4	B 5	B 6	B 7	B 8	B 9
GREEN VEG (1)	1.43	1.92	0.68	1.16	2.31	0.99	0.44	0.50	1.76
WATER (2)	2.03	2.14	2.27	1.49	1.72	1.96			
DRY VEG. (3)	1.92	1.45	2.10	D2.31/2.27	1.72	1.20	0.99	0.85	0.90
CELLULOSE (4)	2.10	1.49	1.93	D2.33/2.27	1.21	1.76	1.01		

(1)   Green Manzanita Leaf (Elvidge, unpublished data)
(2)   Wet cotton cellulose (Elvidge, unpublished data)
(3)   Dry grass - Cripple Creek, Colorado (Kruse, unpublished data)
(4)   Cotton cellulose (Elvidge, unpublished data)

plant biochemistry, health, and productivity (Peterson et al., 1988; Goetz et al., 1990). Measurement of these constituents allows researchers to estimate mass and energy exchange rates and to map subtle changes in ecosystem functioning. Although constituent spectra do have characteristic spectral features that influence the overall reflectance shape, the individual features typically are not readily apparent in the composite vegetation spectra (Goetz et al., 1990). Ongoing research has concentrated on using techniques such as derivative spectroscopy, curve fitting, and spectral unmixing to determine relations between canopy biochemistry and reflectance. The feature extraction and analysis software developed at CSES also provides the potential of being able to directly detect and characterize the individual absorption features caused by the vegetation constituents (Figure 15). Identification of these features could potentially allow remote quantification of canopy level concentrations using imaging spectrometers.

OZONE DAMAGE MAPPING EXAMPLE
CHLOROPHYLL BAND DEPTH/RED EDGE SHIFT

Ustin and Curtiss (1989) have demonstrated that forest decline symptoms caused by air pollution can be detected using reflectance spectroscopy. They used the JPL Portable Instantaneous Display and Analysis Spectrometer (PIDAS) to examine forest decline caused by ozone pollution to Ponderosa Pine (*Pinus ponderosa*) in the southern Sierra Nevada, California. They observed that moderate levels of ozone exposure resulted in needle chlorosis, premature foliar loss, and altered canopy architectures.

To assess the damage, pine needles were clustered according to year of development into "whorls" and ozone damage was visually estimated based on the presence of chloritic banding and mottling. Chlorophyll a, b, and total chlorophyll were determined for each whorl for two sites (sites 12 and 14, Ustin and Curtiss, 1989). Both sites were rated as moderately damaged by ozone with site 12 having a slightly higher damage rating than site 14 (75% vs 60% of branches with chlorotic mottle or banding). Reflectance spectra of uniformly bundled packets of needles were measured for each whorl age from 0.40 to 2.45 μm using the PIDAS. It was observed that ozone damage appeared to increase with the age of the whorl, and that the position of the reflectance "red edge" inflection point near 0.70 μm shifted to shorter wavelengths with increasing damage (decreased chlorophyll concentrations). Similar observations of the red edge shift have been reported by Collins (1978), Chang and Collins (1983), and Rock et al. (1988).

Brian Curtiss (CSES/University of Colorado) provided us with the PIDAS digital spectral data to test weather the feature extraction and absorption band characterization software we have developed for mineral analysis would be able to detect the vegetation spectral changes caused by the ozone damage. Figure 16 shows the Ponderosa Pine reflectance spectra from 0.50 to 0.80 μm. Note that in general, it can be observed that the older whorls (higher whorl number) have higher reflectance in the 0.67 μm region, however, the depth of the band and the position of the "red edge" visually appears very similar for all spectra. Previous assessments of vegetation health and vigor have relied on detecting this very small shift in the position of the red edge, however, it is not clear weather this shift will be observable using imaging spectrometers such as AVIRIS and HIRIS. After applying the continuum removal and feature extraction procedures to the spectral data, the

34

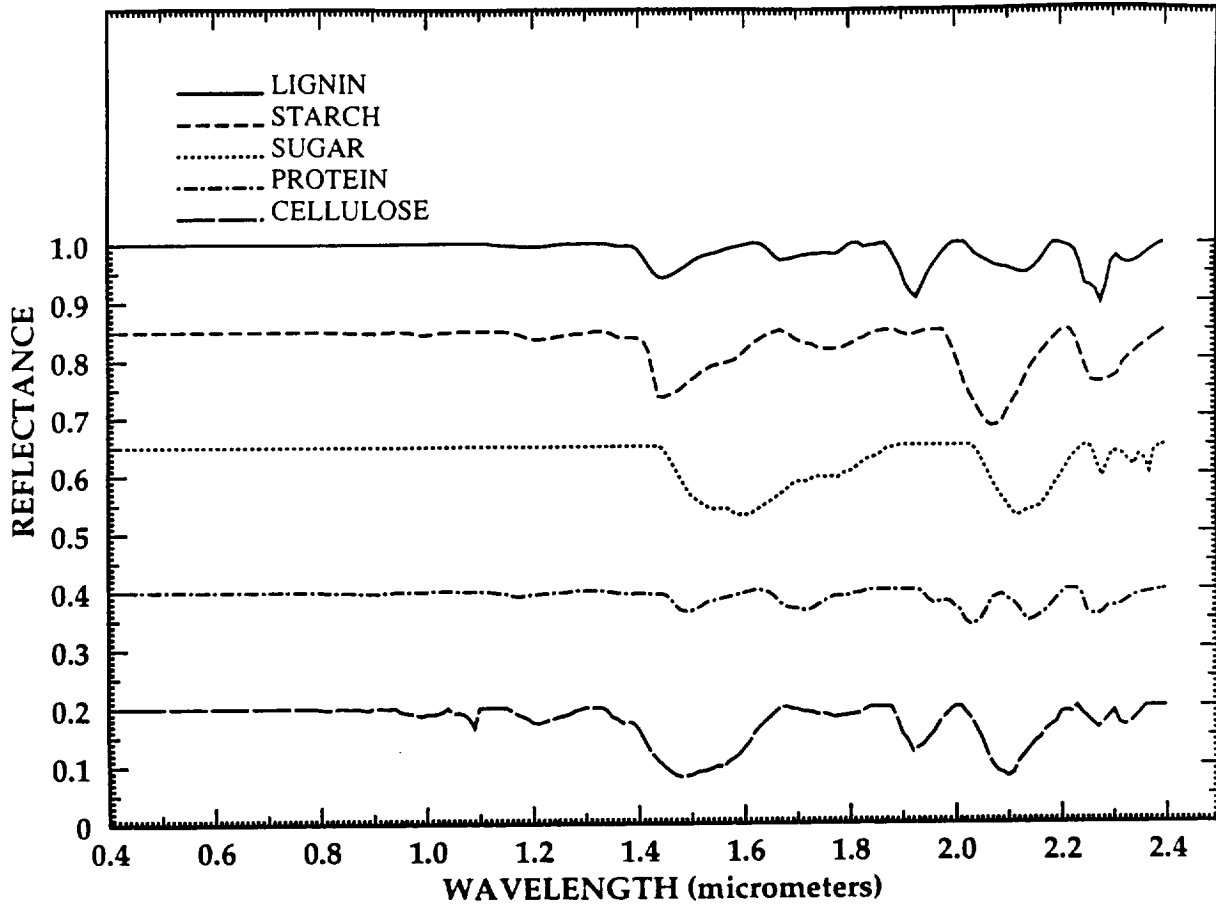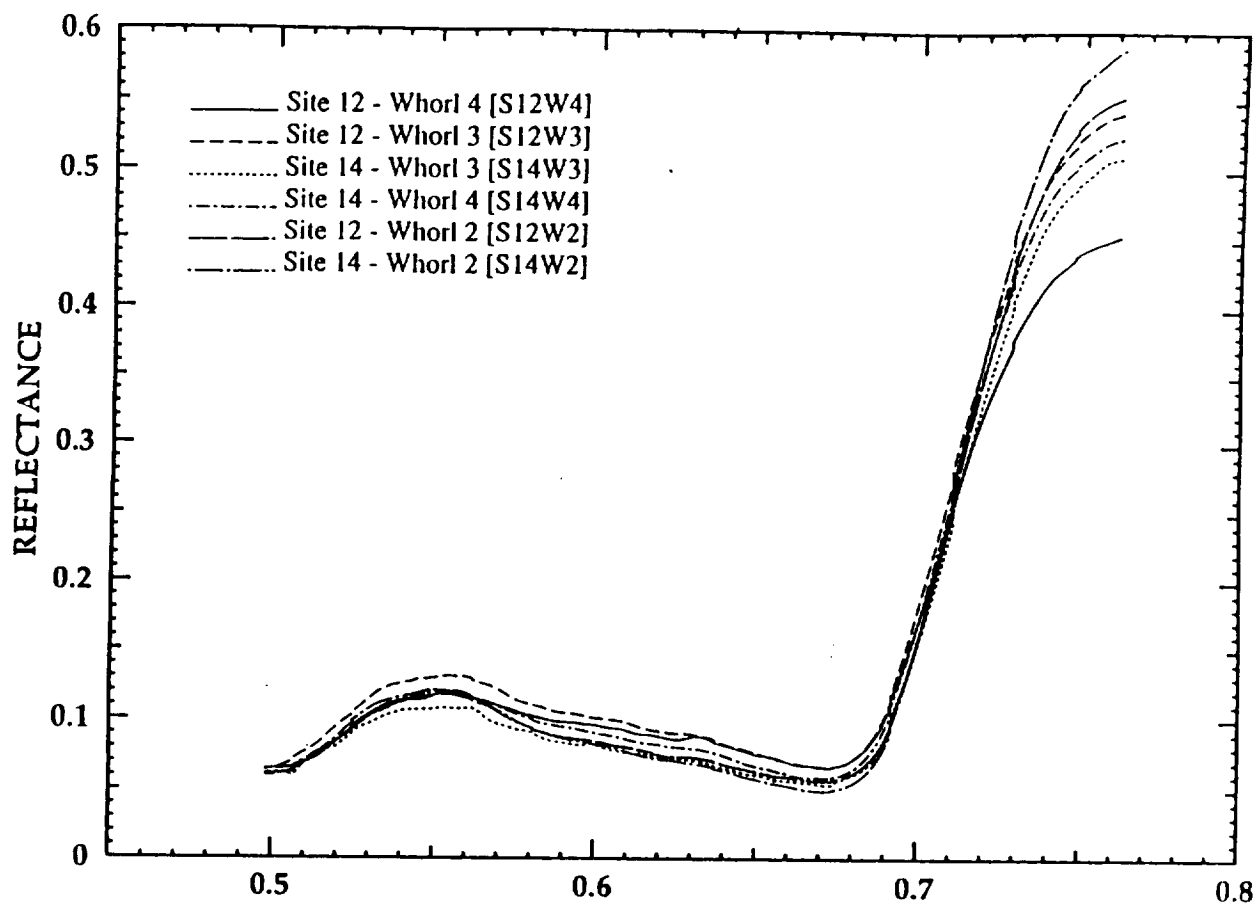Figure 15.   Continuum-removed vegetation constituent spectra.

35

Figure 16.   PIDAS reflectance spectra of moderately ozone-damaged ponderosa
pine from site 12 and 14 of Ustin and Curtiss (1989).

relationship between the whorl age and the reflectance spectra is much clearer (Figure 17). The whorl age is seen to be closely related to the depth of the absorption feature at 0.67 μm. This feature can be directly related to the chlorophyll concentration in the vegetation (Salisbury and Ross, 1969; Thomas and Oerther 1972; Tsay et al., 1982; Ustin and Curtiss, 1989). This observation is confirmed by the very high linear correlation $R^2=0.985$) between the depth of the 0.67 μm absorption feature as calculated by the feature analysis software and the total dry weight chlorophyll concentrations as measured by Ustin and Curtiss (1989((Figure 18). The band width at half the absorption feature depth (FWHM) is also closely related to the chlorophyll content ($R^2=0.82$). Although these results look promising, further study needs to be done to assess the feature extraction procedures for other vegetation types, for actual imaging spectrometer data, and the effects of other stresses on the spectral feature characteristics of vegetation. We conclude from the ozone data, however, that the feature extraction procedure does provide a means of estimating ecosystem parameters and that rules could be developed to do this automatically with the expert system for imaging spectrometer data.

MINERALIZATION STRESS - CCRS EXAMPLE

Chlorophyll is the major photosynthetic pigment in higher plants. Major chlorophyll absorption features occur between 0.56 and 0.67 μm (Figure 12). Stress in plants can result in chlorosis (chlorophyll loss). This phenomenon has been documented in reflectance spectra as a shift in the "red edge" (Gates et al., 1965; Collins, 1978). Stress-induced shifts in the red edge have been reported both toward longer (red) and shorter (blue) wavelengths, and have been attributed to changes in chlorophyll concentration. Ustin et al. (1988) and Curtiss and Ustin (1989) indicate that although the red edge is, in part, controlled by chlorophyll concentration, it is also influenced by the condition of the chloroplast membranes on which the chlorophyll is bound. They attribute broadening of the the chlorophyll absorption bands to disruption of the membranes. It is suggested that the position of the red edge shifts to either red or blue wavelengths depending on whether the membrane disruption or the chlorophyll loss process dominates.

Our work with spectra of Curtiss and Ustin's ozone damaged Ponderosa Pine indicated, that at least for that species, direct measurement of the depth and width of the chlorophyll absorption band was an excellent means of estimating chlorophyll content ($R^2=0.985$, N=6). Ustin and Curtiss' correlation of chlorophyll concentration and the red edge was considerably lower ($R^2=0.72$, N=107). Although some of this difference may be due to scatter caused by the difference in sample size, our research suggests that directly characterizing the absorption band itself rather than a subtle shift in the absorption edge may be a better indicator of the vegetation stress exhibited as chlorophyll loss.

During 1990 we attempted to verify these direct indicators of vegetation stress using laboratory spectra. Digital spectra for trees from the Canadian boreal forest were obtained as part of the IGCP spectral database collection effort. Spectra were provided by Dr. Vernon Singhroy of the Canadian Center for Remote Sensing (CCRS) for trees growing both on non-mineralized and mineralized ground (areas with anomalous concentrations of various metals). These spectra were analyzed using the feature extraction procedures designed for the expert system to verify the procedures' applicability to assessment of vegetation parameters. Based on our

Figure 17. Continuum-removed PIDAS spectra of ozone-damaged ponderosa pine. Note decreased absorption band depth of more severely damaged, older growth (whorls 2, both sites).

**0.67 BAND DEPTH
VS TOTAL CHLOROPHYLL**

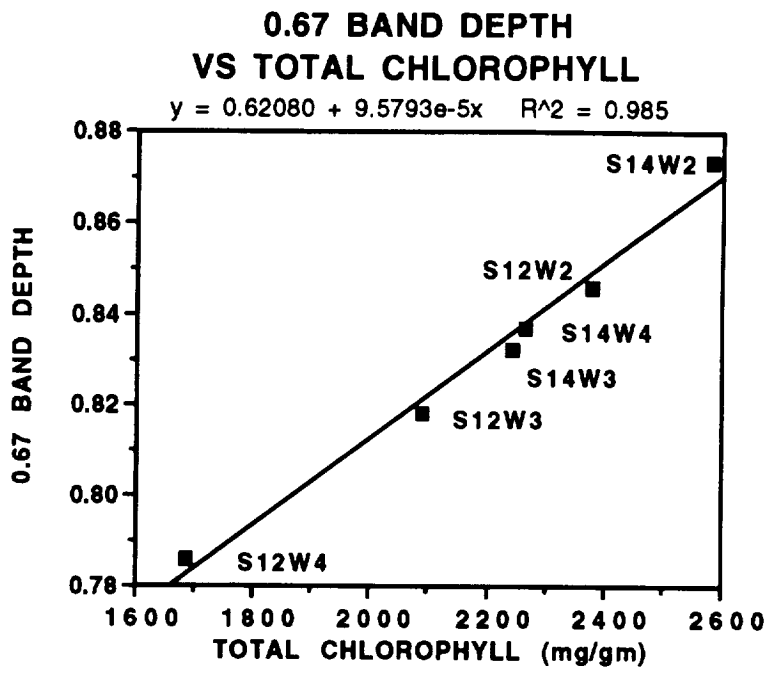$y = 0.62080 + 9.5793e\text{-}5x \qquad R^2 = 0.985$
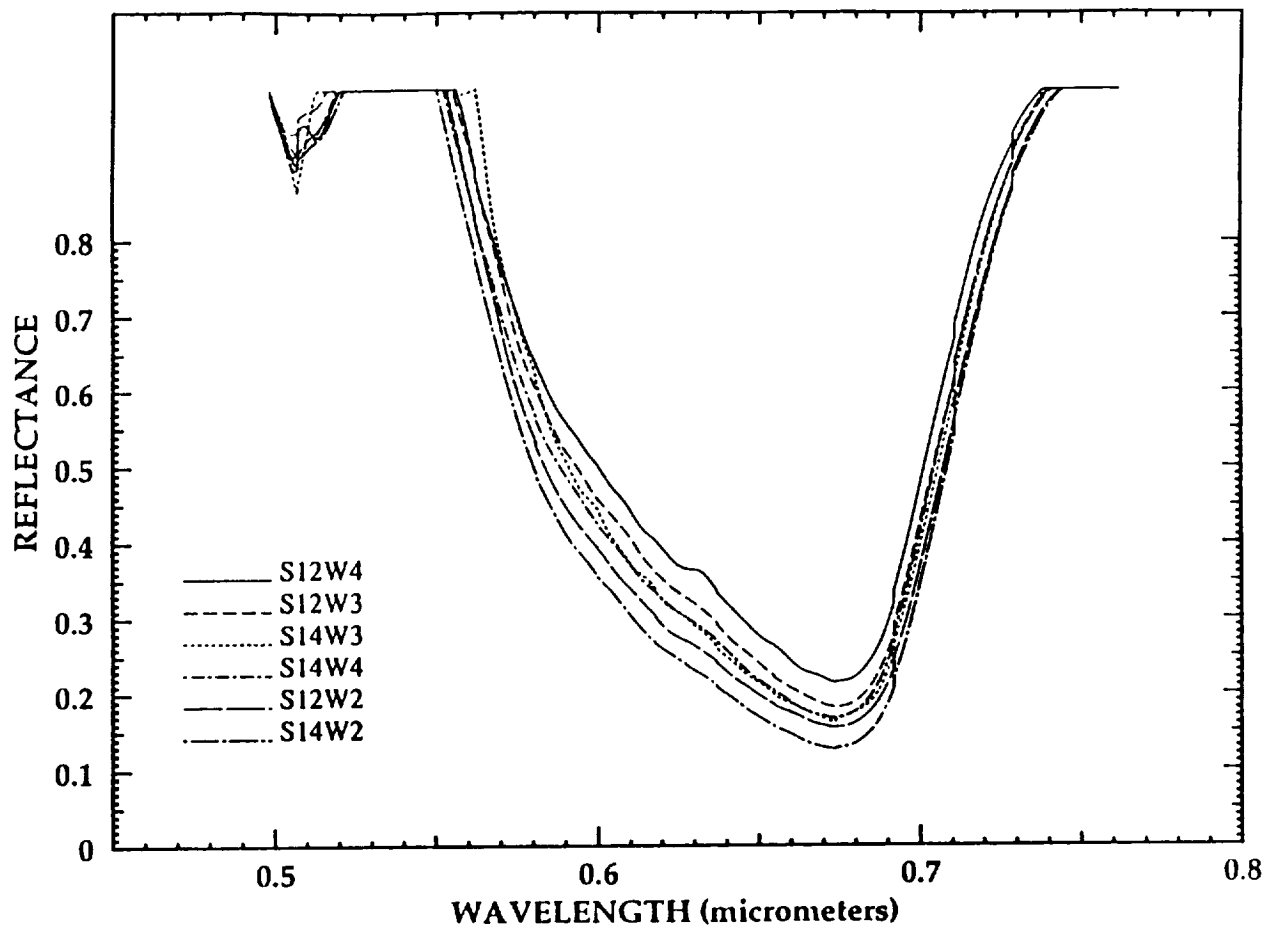
Figure 18. Correlation of 0.67 absorption band depth with total chlorophyll for whorls 2 through 4 at sites 12 and 14 of Ustin and Curtiss (1989).

experience during 1989 with the ozone-damaged Ponderosa Pine needles, which showed a high correlation between total chlorophyll and the 0.67 μm absorption band depths and widths, we expected that we would be able to detect and characterize any damage or stress caused by the exposure to mineralized soils.

The average of 10 spectral measurements for five species of trees were evaluated for both non-mineralized (background) and mineralized samples. Figure 19 shows an example of both the background and mineralized reflectance spectra for one species of trees. The red edge shift for this example is very small. When the feature extraction procedures are used to characterize the chlorophyll absorption feature near 0.67 μm the trend is similar to that for decreased chlorophyll shown previously for ozone damaged Ponderosa Pine. This trend is consistent across several species, including both evergreen and deciduous types (Figure 20a). In addition, 0.67 μm absorption band width (FWHM) is also a good indicator of vegetation stress (Figure 20b). The FWHM decreases with stress for four of the five species. Chlorophyll absorption band depth and width could be used in combination to develop field and aircraft techniques for characterization and quantitative mapping of vegetation stress. This example clearly demonstrates that the feature extraction and absorption band characterization procedures developed for analysis of mineral spectra are applicable to analysis of vegetation spectra.

EXPERT SYSTEM DEVELOPMENT
GENERAL
The final stage of this research applied the feature extraction procedure to field, laboratory, and aircraft spectra. The expert system was operational for single spectra prior to the start of NASA funding in 1989 (Kruse et al., 1988). The original version ran under the VAX VMS operating system on DEC MICROVAX computers. This research extended these procedures to UNIX-based computers and to complete imaging spectrometer data sets.

Initially, FORTRAN was used to implement the feature extraction procedures. Critical absorption band characteristics for a given mineral were defined by manually analyzing the feature extraction results and comparing to published reflectance spectra. The PROLOG programming language (Quintus Computer Systems, 1987) was used to implement the facts and rules Prolog simplified logical structuring of the program to model the decision processes followed by an experienced analyst. A tree hierarchy was used to reduce analysis time (Figure 21). A decision was made at each level of the tree based on facts and rules derived through prior analysis of the spectral library (Figure 22).

The decision process used by the computer was designed to emulate the logical steps followed by an experienced analyst. The strongest absorption feature for a given spectrum was determined, and the spectrum broadly classified (eg. clay, carbonate, iron oxide). Primary band characteristics (eg. doublet, triplet) and secondary/tertiary absorption bands were used to progress through the tree structure until an identification was made. If the decision process failed because there was insufficient information to identify a specific mineral, then the last classification was used to give the best answer possible.

Re-evaluation of the procedures and a major revision of the software was started in February 1989 based on poor speed performance, lack of determinative

Figure 19. **A.** Reflectance spectra for White Birch; **B.** Reflectance spectra for Black Spruce; **C.** Continuum-removed spectra for White Birch; **D.** Continuum-removed spectra for Black Spruce. Note position of red edge inflection in A and B for trees growing on both background and mineralized areas. Note differences in absorption band depth and width in C and D.
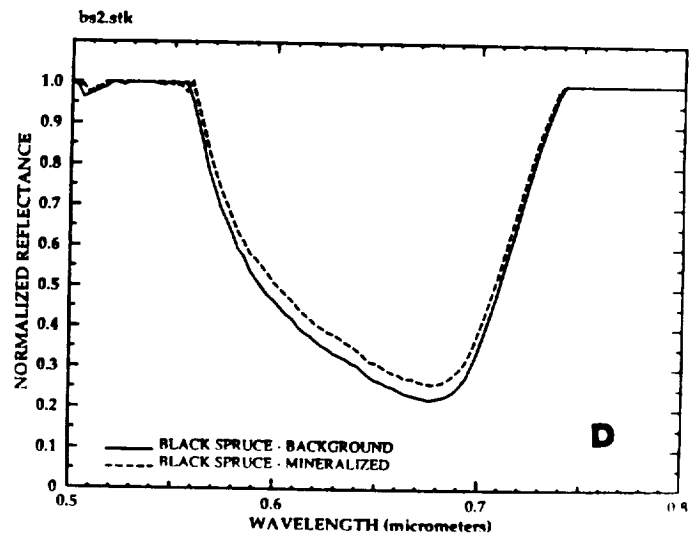
Figure 20a. Plot showing relationship of 0.67 µm absorption band depth to vegetation stress. Absorption band depth for plants growing on mineralized soil is less than that for plants growing on background soil for all five species.

VEGETATION STRESS
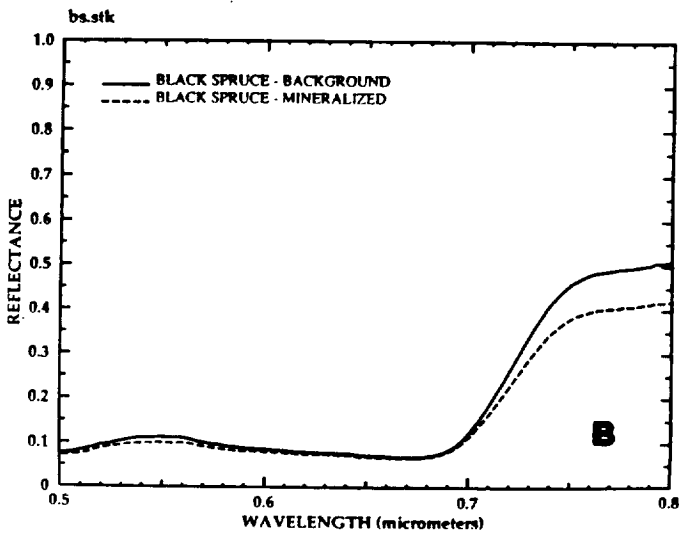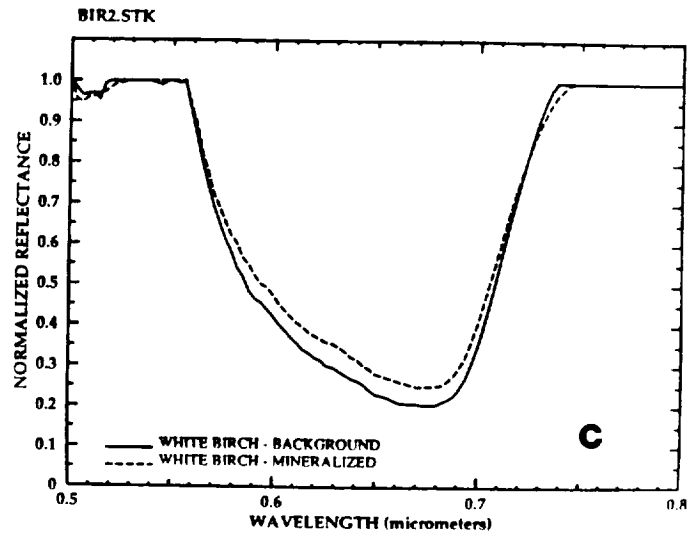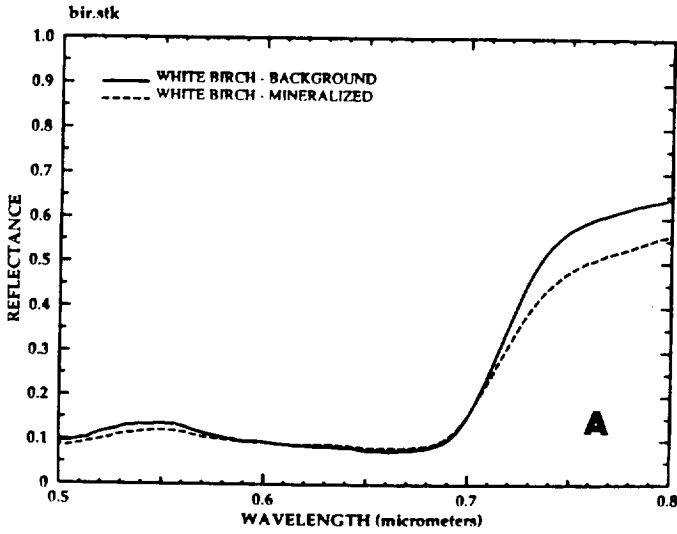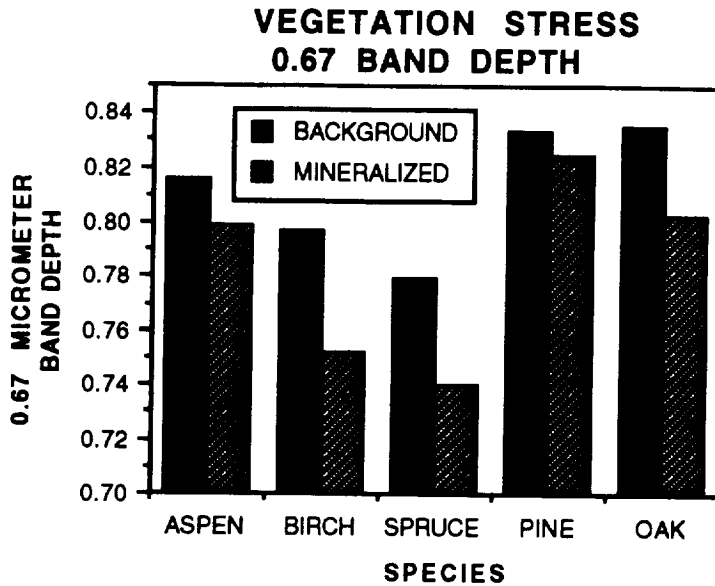**0.67 BAND DEPTH**

Figure 20b. Plot showing relationship of 0.67 µm absorption band width (FWHM) to vegetation stress. Absorption band FWHM for plants growing on mineralized soil is less than that for plants growing on background soil for four of five species. There was no change in FWHM for white birch.

VEGETATION STRESS
0.67 BAND WIDTH

42
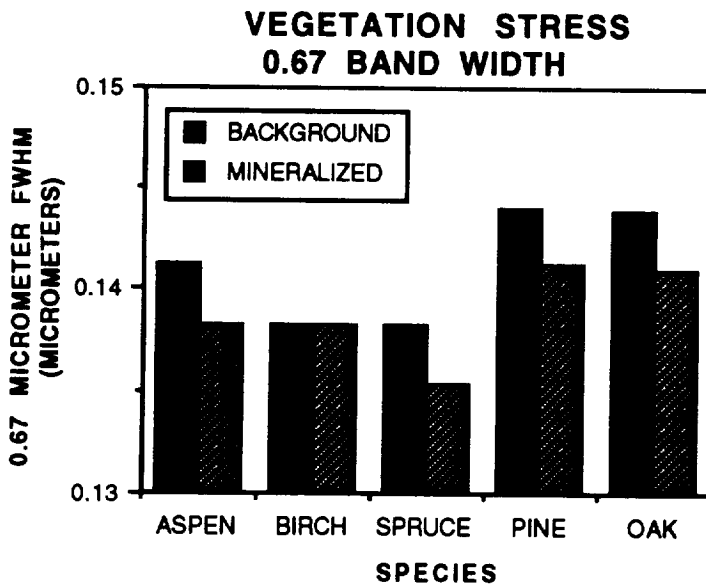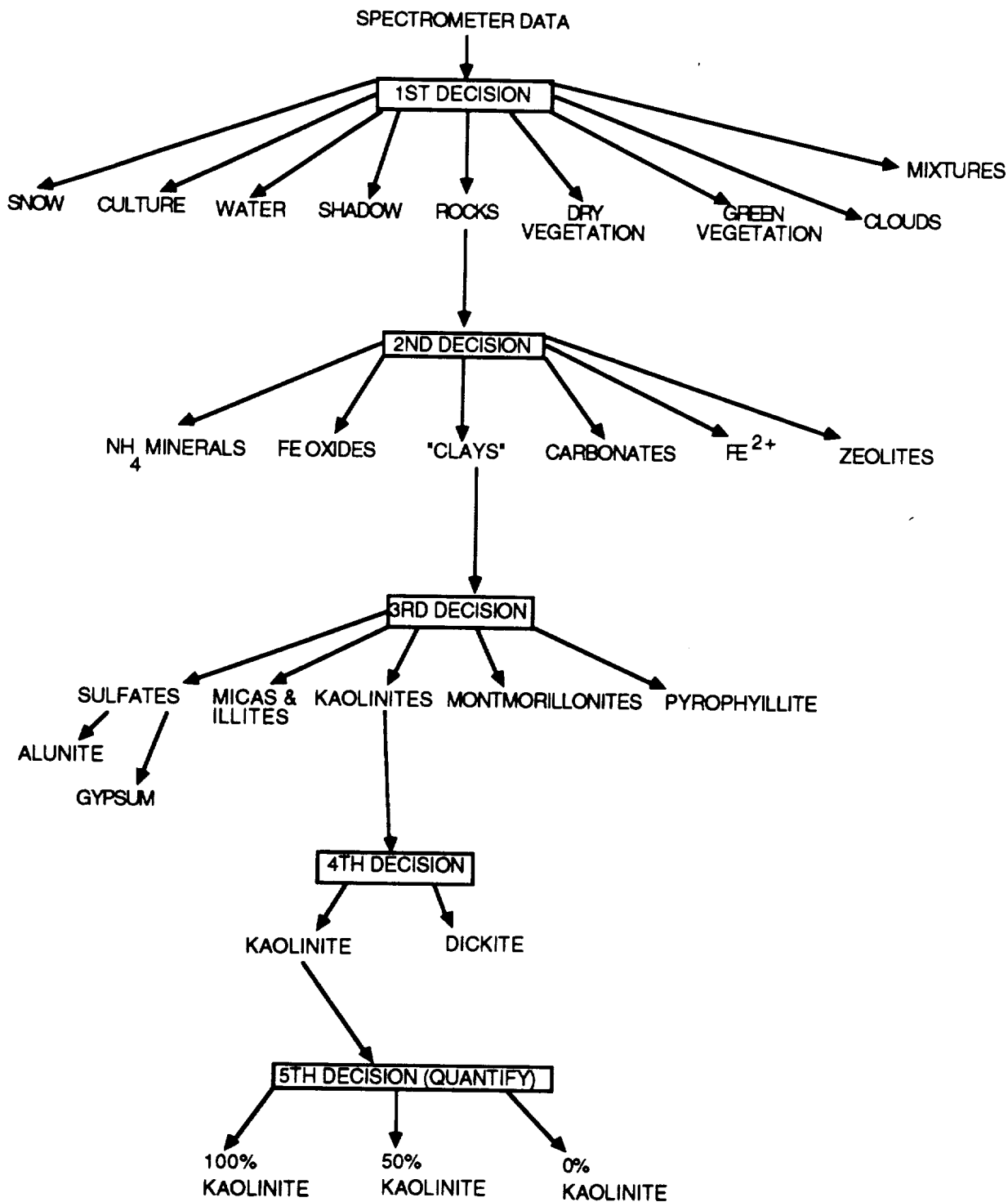
Figure 21.   Tree hierarchy for expert system

Figure 22.   Example of rules: kaolinite vs. alunite.

<u>1st Decision</u> (Surface class)
if not strong band near 0.67 µm
<u>and</u> **if not** broad spectral bands near 1.4 and 1.9 µm (vegetation)
then look for in rock class

2nd Decision (rock level)
if it has a deep band in 2.15-2.22 µm region
then look for in "clay" species.

3rd Decision ("clay" species)
if it has a doublet near 2.2 µm
<u>and</u> strongest band of the doublet is 2.21 µm
<u>and</u> weakest band of the doublet is near 2.17
<u>and</u> 2.21 µm asymmetry is <<1 (Left Asymmetry)
<u>and</u> 2.17 µm asymmetry is >>1 (Right Asymmetry)
<u>and</u> additional smaller bands near 2.32, 2.36, and 2.38 µm
then it is **kaolinite**.

if it has a broad band near 2.17 µm
<u>and</u> a weak shoulder near 2.21
<u>and</u> 2.17 µm asymmetry is <<1 (Left asymmetry)
<u>and</u> additional weaker bands near 2.32 and 2.42 µm
then it is **alunite**.

mineral identification by the prototype expert system, and the receipt of funding from NASA for the project. We made the decision to convert all of the software to the C programming language to increase the efficiency, portability, and speed of execution.

It was also clear that noisy data typical of most aircraft systems was going to present severe problems to a system that relied only on identification of specific mineral absorption features. We were familiar with the binary encoding schemes successfully used for analysis of NASA Airborne Imaging Spectrometer data (Mazer et al., 1988) and so decided to try to incorporate this feature as part of the expert system analysis. Figure 23 shows the expert system analysis procedure revised to include binary encoding in the decision process.
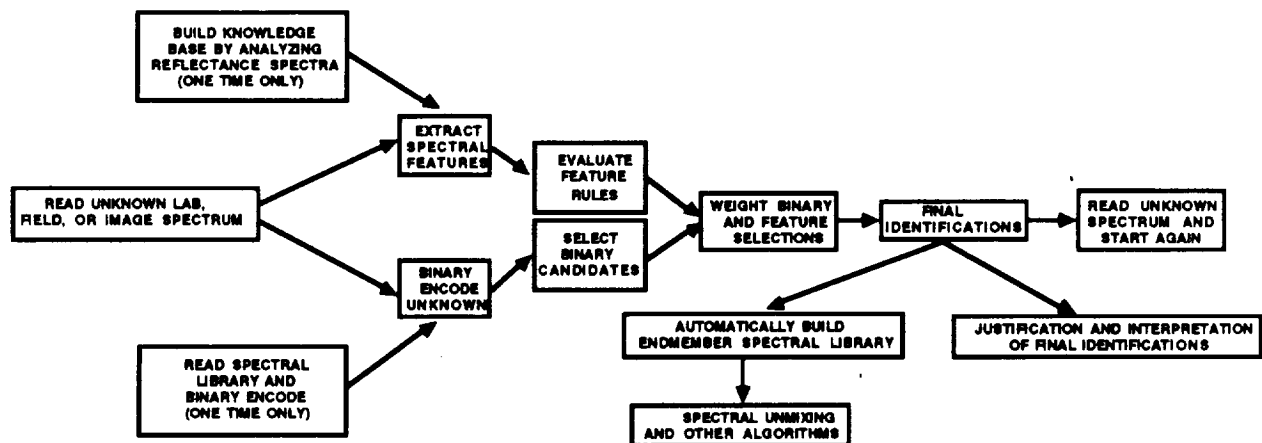
Figure 23.   Revised expert system analysis procedures

SINGLE SPECTRUM ANALYSIS
Example for Laboratory Spectrum

The stand-alone user interface for the expert system for analysis of individual spectra was improved to provide a complete report on the decision process, including justification. Figure 24 is an example of the results of the step-by-step analysis procedure used to determine mineralogy. It shows an analysis of a laboratory calcite spectrum using the expert system. The results of the feature extraction procedure and absorption band parameter extraction are shown in Figure 24a. The interaction of the absorption features and the rules result in the broad classification shown in Figure 24b. Note ambiguities caused by shared spectral

Figure 24. Expert system analysis of calcite lab spectrum (From Kruse et al., 1990a).

24A. FEATURE ANALYSIS:

BAND	ORDER	WAVE(μm)	DEPTH	FWHM	ASYM
1	1/1	2.340	0.3001	0.0980	0.3047
2	1/1	1.997	0.0788	0.0490	0.5154
3	1/1	1.870	0.0603	0.0490	0.6033
4	1/1	2.164	0.0452	0.0392	0.1947

24B. EXPERT SYSTEM BROAD CLASSIFICATION:

There are features from:
    vegetation
    carbonates
    clays
    micas and illites
    calcite

24C. BINARY ENCODING MATCHES (percentage):

Buddingtonite	85.24	Kaolinite	80.00
Montm	82.86	Pyrophyllite	83.33
Illite	35.71	Muscovite	56.19
Alunite	74.76	Gypsum	65.71
Epidote	53.81	Chlorite	40.95
Calcite	100.00	Dolomite	86.19
Actinolite	52.38	Tremolite	84.29
Jarosite	58.10	Hematite	53.81
Goethite	56.67	Green Vegetation	58.10
Dry Grass	73.33		

24D. CALCITE FINAL RESULTS - WEIGHTED DECISION:

According to the expert system and the binary encoding
performed on the spectrum, the probability of the presence of:

    Calcite is nearly certain
    Dolomite is medium
    Buddingtonite is medium
    Muscovite is medium

24E. JUSTIFICATION - CALCITE:

The binary match to calcite is 100.00 % so
the binary match is rated very high
The carbonate feature between 2.30 and 2.35 μm is present
The calcite feature at 2.34 μm is present
The overall expert guess for the probability of
calcite is **Nearly Certain**

24F. JUSTIFICATION - DOLOMITE:

The binary match to dolomite is 86.19 % so
the binary match is rated high
The carbonate feature between 2.30 and 2.35 μm is present
The dolomite feature at 2.32 μm is not present
The overall expert guess for the probability of dolomite is **Medium**

characteristics. Figure 24c shows the percentage match of the spectrum with the binary library. Note the 100% match between the library calcite and the unknown spectrum. This is because this particular calcite spectrum comes from the library. Figure 24d shows the final result of the decision process when the binary encoding is used to weight the feature extraction process. Figures 24e and 24f show the justification for the identification of calcite versus dolomite.

Alunite, Kaolinite, Buddingtonite from GERIS data

The refined feature extraction algorithms and expert system were tested on individual spectra from Geophysical and Environmental Research Inc. 64 channel imaging spectrometer (GERIS) data of Cuprite, Nevada. This instrument is the first commercial imaging spectrometer. The GERIS collects data from 0.43 to 2.5 μm in 64 channels of varying width. The 24 visible and infrared bands between 0.43 and 0.972 are 23 nm wide, the 8 bands in the infrared between 1.08 and 1.8 μm are 120 nm wide, and the 31 bands from 1.99 to 2.5 μm are 16 nm wide (William Collins, written communication, 1988). Only the last 31 bands were used in this study. The feature extraction procedures were used to extract absorption band characteristics directly from the image data. The expert system successfully identified the minerals kaolinite, alunite, and buddingtonite from the data. These minerals had previously been identified manually and verified through field checking, laboratory spectroscopy, and XRD analysis (Kruse et al., 1988, 1990b).

Hematite, goethite, sericite, calcite, and dolomite from AVIRIS data

The continuum-removal and feature extraction procedures were also used to analyze individual spectra from AVIRIS data for a site in the northern Grapevine Mountains, Nevada (Kruse, 1988; Kruse et al., 1988, 1993a). Individual spectra were extracted from the AVIRIS data for known occurrences of hematite, goethite, sericite, calcite, and dolomite. Comparison of the shapes and positions of the absorption features with laboratory spectra made positive identification of the minerals possible. The AVIRIS data not only allowed identification of the carbonate-group-minerals, but permitted identification of the individual species (calcite and dolomite) based upon a 20 nm (2 channel) difference between the position of the main absorption feature (2.34 vs 2.32 μm). The feature extraction procedures successfully produced continuum-removed spectra that show this offset. Spot checking of the imaging spectrometer data for areas of known mineralogy showed a good match between extracted absorption features, laboratory measurements, and the expert system's automated identification The feature extraction procedures successfully produced continuum-removed spectra that could be compared to laboratory spectra. The strongest absorption bands corresponded to bands in the laboratory spectra and the prototype expert system correctly identified the minerals hematite, goethite, sericite, dolomite, and calcite.

IMAGE ANALYSIS

The final step in developing a generalized expert system for the analysis of imaging spectrometer data was to map the spatial distribution of the minerals using the expert system. Because of the association of a spectrum with each pixel of the image, implementation of the expert system consisted of applying the single spectrum analysis to each pixel (~300,000). The analysis was segmented, with

47

production of several intermediate image cubes to allow testing and evaluation of each step. Interactive viewing of the derived cubes was used to verify results.

The expert system as described above was tested on several imaging spectrometer data sets including images from northern Death Valley, California; Paradise Peak, Nevada; and the Drum Mountains, Utah. It has been proven as the first, automated step in a complete scheme for quantitative analysis of imaging spectrometer data (Kruse et al., 1993a; Kruse and Lefkoff, 1993).

AVIRIS is the first of a second generation of imaging spectrometers measuring near-laboratory quality spectra in 224 10 nm-wide channels in the spectral range 0.41 to 2.45 μm (Porter and Enmark, 1987). The AVIRIS is flown aboard the NASA ER-2 aircraft at an altitude of 20 km, with an instantaneous field of view of 20 m and a swath width of about 10 km. It utilizes four linear arrays and four individual spectrometers to collect data simultaneously for the 224 bands in a scanned 614 pixel-wide swath perpendicular to the the aircraft direction. The second dimension of the images is provided by the forward motion of the aircraft, which moves the ground field of view along the terrain.

The expert system requires that the imaging spectrometer data be calibrated to reflectance because the rules are built using laboratory reflectance spectra. Once the data are properly calibrated, the expert system analysis proceeds in the same fashion as for a laboratory spectrum. Each pixel in the image is in effect a single spectrum. The procedure then is to treat each pixel individually and sequentially to remove the continuum, extract the features, and compare the features to the feature rules built from the spectral library. A match occurs when all of the attributes of a fact from the input spectrum fall within the user defined tolerances of a rule's attributes. The result of the rule-based matching is a certainty probability value between 0.0 and 1.0 corresponding to the sum of the weights of the matching rules divided by the sum of the weights of all of the rules for the selected endmember. For example, as described previously, if a specific mineral was expected to have three absorption features with respective weights of 1.0, 0.6, and 0.3 (must-have, should-have, and may-have) and it only had two of the features (say the 1.0 and the 0.3 features) then the probability of occurrence of that specific mineral could be represented as $(1.0+0.3)/(1.0 + 0.6 + 0.3) = 0.68$. The value "0.68" would be assigned to a pixel in the output image for that mineral. The result of these analyses for the imaging spectrometer data is a new "information cube" consisting of the certainty probability displayed as a single gray-scale image for each endmember contained in the spectral library (Figure 25). These images contain the certainty probability value for each pixel (between 0.0 and 1.0) indicating the degree of match to the feature rules.

In practice, as described previously, because present imaging spectrometers do not have adequate signal-to-noise (SNR) performance, a perfect match to the rules is rare. Implementation of additional noise-tolerant techniques is usually required to assist the feature based methods. Binary encoding was used here in the same fashion as for the single spectrum case to provide additional spectral information. The result of the binary encoding analysis for the imaging spectrometer data is a new information cube consisting of the degree of binary match displayed as a single gray-scale image for each endmember contained in the spectral library (Figure 26). With noisy data, it is necessary to combine the binary results and the rule-based results to accurately identify materials. The final match for each endmember

Figure 25. Gray-scale mineral maps showing expert system results for selected minerals. The gray scale shows the degree of match to only the feature analysis results, with the brightest pixels representing greater degree of certainty, and thus good matches to the library spectra.
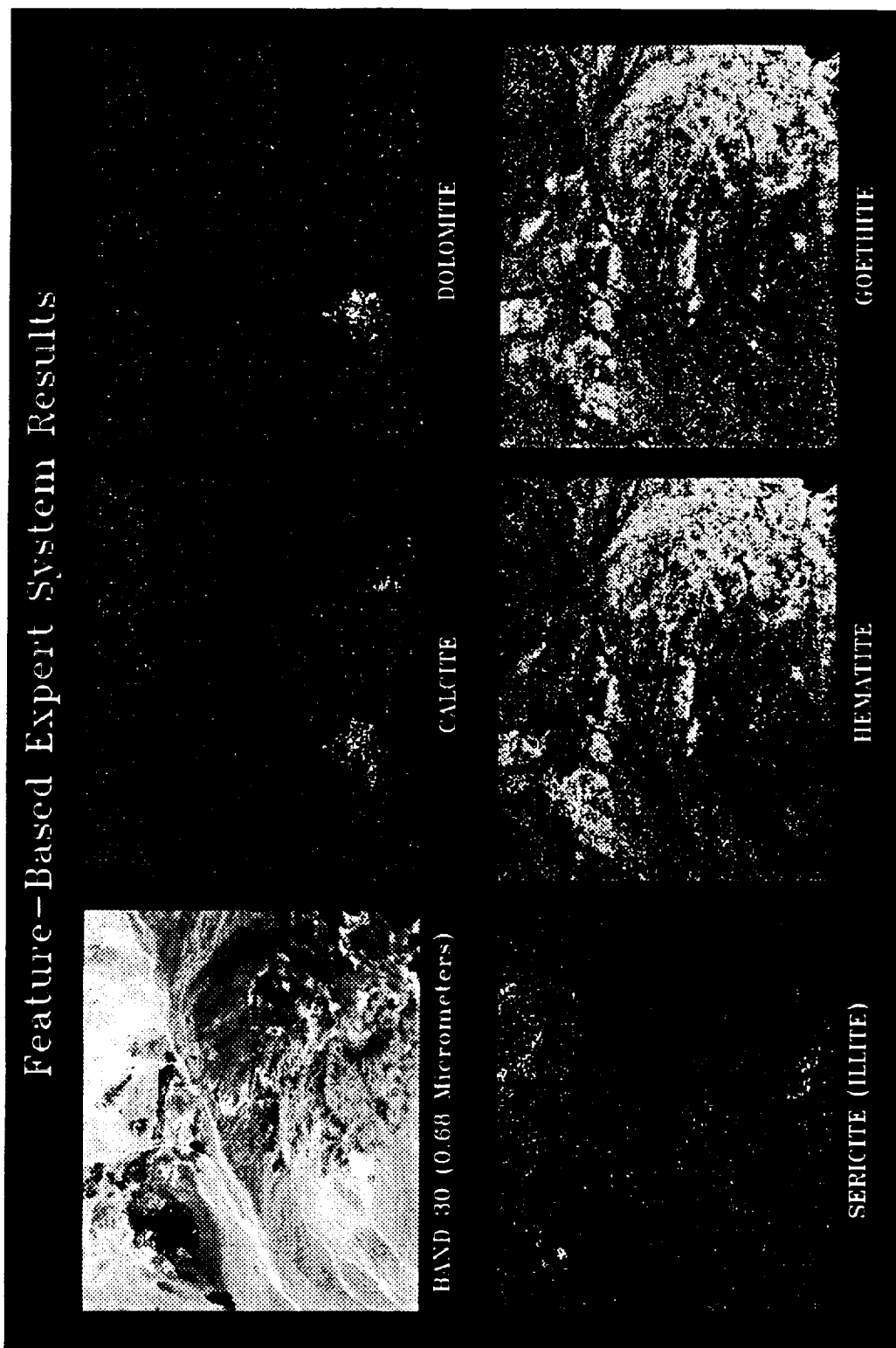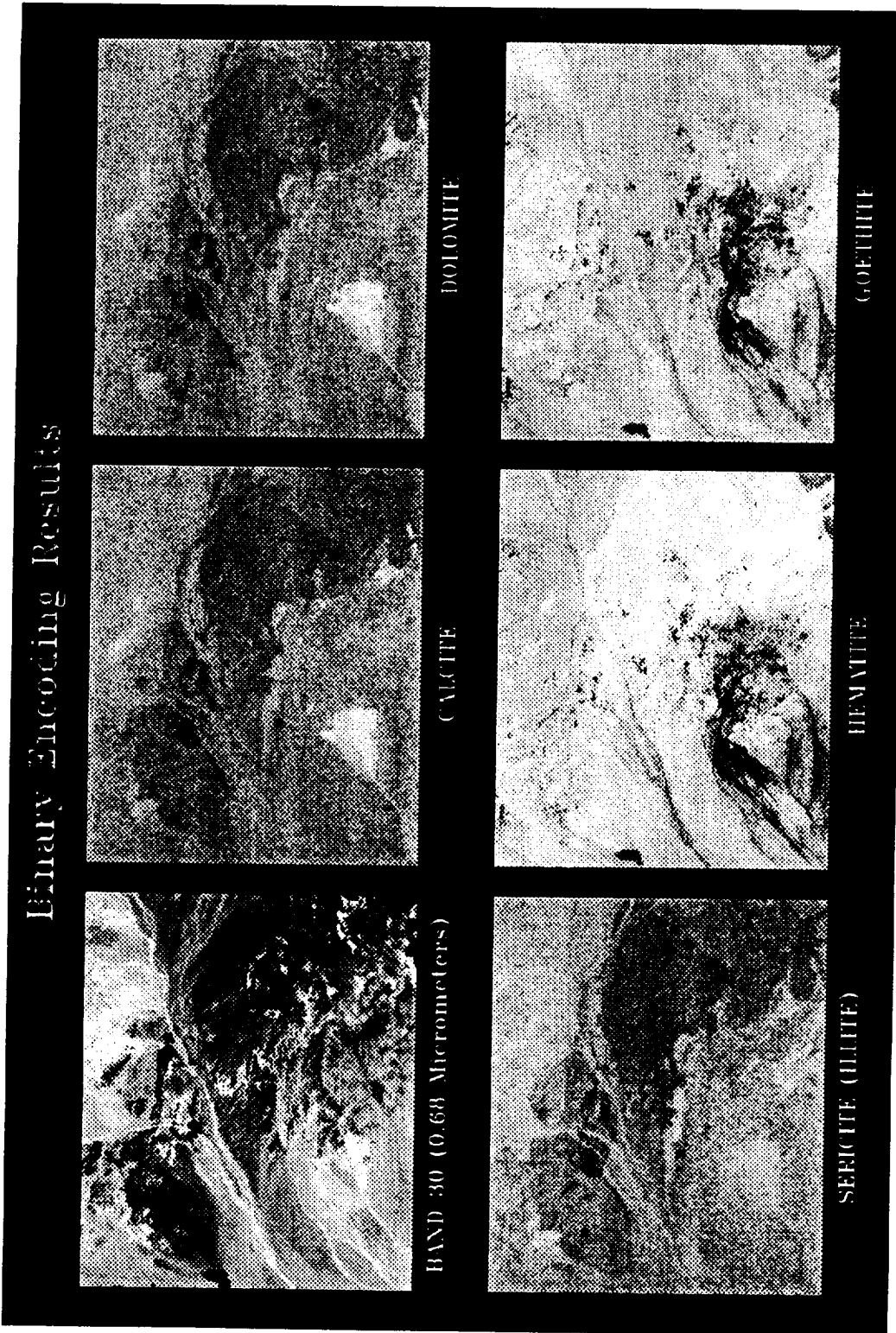
Figure 26. Gray-scale mineral maps showing expert system results for selected minerals. The gray scale shows the degree of match to only the binary encoding analysis results, with the brightest pixels representing greater degree of match to the library spectra.

spectrum is typically calculated by weighting the binary results at 40% and the rule-based results at 60%. The user can also select other weighting factors depending on the quality of the data. Noise-free data would ideally use only the absorption feature rules. The result of the weighted decision is a certainty probability between 0.0 and 1.0 (again presented as an information cube) describing how certain the expert system is that the given input spectrum matches a given endmember spectrum. Figure 27 shows a schematic of the final information cube combining the combined binary/feature expert system analysis. The final expert systems results cube also contains a "best endmember" image assigning the expert system's best guess of the predominant mineralogy for each pixel based upon the highest certainty probability. Saving of additional image cubes containing the continuum-removed spectra and the absorption feature attributes (facts) are optional as is the automatic calculation of average spectra for the endmembers identified (an endmember spectral library) (Kruse, 1992a)

Although this expert system concept has been under development for some time, a recurring problem was the lack of software tools to display the results and evaluate them in the geologic context. Several tools were therefore developed as part of this research for general viewing and analysis of imaging spectrometer data and specifically for viewing the expert system results. The Spectral Image Processing System (SIPS) is one example of this software that has already been released to organizations outside CSES (Kruse et al., 1993b). Another tool, the "General Use Expert System for Spectra (GUESS)" is a tool more specifically designed for analysis of the expert system analyses described above (Lefkoff and Kruse, 1993). It provides interactive capabilities for evaluating expert system performance. Figure 28 shows the results of the expert system analysis of AVIRIS data for the area in northern Death Valley, Nevada, for the mineral dolomite. This tool displays an AVIRIS image with all pixels matching the dolomite binary encoding and feature rules color coded as black. These pixels represent 20 m x 20 m areas on the ground where dolomite is the predominant mineral and generally correspond in location and pattern to field-mapped geology and field spectral measurements (see Kruse, 1988). Also displayed are two AVIRIS spectra extracted for the 87 and 75 percent certainty probability levels (16 and 791 pixels respectively) for dolomite showing the characteristic absorption features near 2.32 µm. The similarity of pixels displayed on the image can be controlled using the slider to change the certainty probability level. As the certainty is decreased, more pixels are displayed, however, the spectra are less similar to the dolomite lab spectrum used to derive the rules. Figure 29 shows an endmember spectral library extracted from the imaging spectrometer data based upon the results of the expert system analysis. These spectra form the starting point for other, quantitative techniques requiring spectral endmembers such as spectral unmixing (Boardman, 1989).

IV. CONCLUSIONS

An expert system has been developed that allows automated analysis of imaging spectrometer data. The key elements consist of automated extraction of spectral features from a spectral library, automated determination of facts from the extracted features, interactive selection of rules for each mineral, and automated decisions concerning mineralogy based on the rules. The result of these analyses is an information cube containing a measure of the certainty of occurrence for each

BAND ATTRIBUTES
POSITION
DEPTH
WIDTH
ASYMMETRY

CUBE OF
ABSORPTION
BAND
ATTRIBUTES

CUBE OF
BINARY
MATCHES

EXPERT
SYSTEM
ANALYSIS

IDENTIFICATIONS
MINERAL A
MINERAL B
MINERAL C
⋮
MINERAL Z
VEGETATION

INFORMATION
CUBE

CERTAINTY
PROBABILITIES
1.0 NEARLY CERTAIN
VERY HIGH
HIGH
MEDIUM HIGH
MEDIUM
MEDIUM LOW
LOW
VERY LOW
0.0 NOT LIKELY
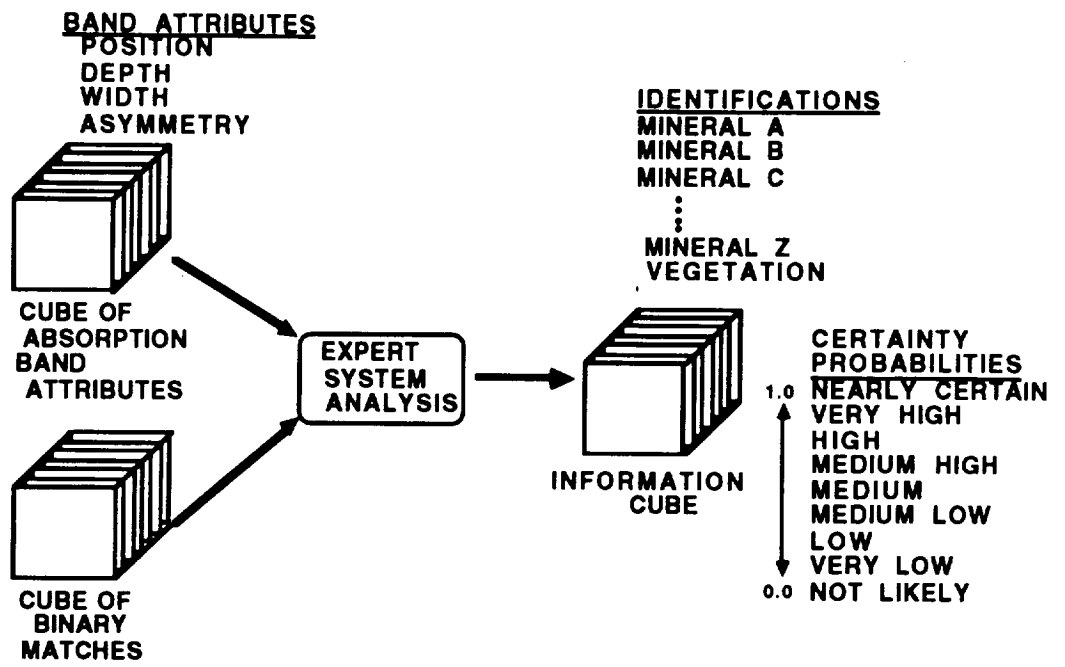
Figure 27   Diagram showing the information cube concept.

Figure 28. Unix screen dump showing a software tool for analysis of the expert
system results. Black pixels (normally red on the CRT monitor) in the
lower center of the image (13704 total) represent areas identified as
dolomite using the combined binary encoding and feature based rules.
Spectra shown are averages for different certainty probability levels.

Figure 29. Expert system-derived endmember spectral library from the northern Death Valley AVIRIS data. From top to bottom these spectra represent average image spectra of muscovite, dolomite, and calcite at the 50% certainty level (From Kruse and Lefkoff, 1992).

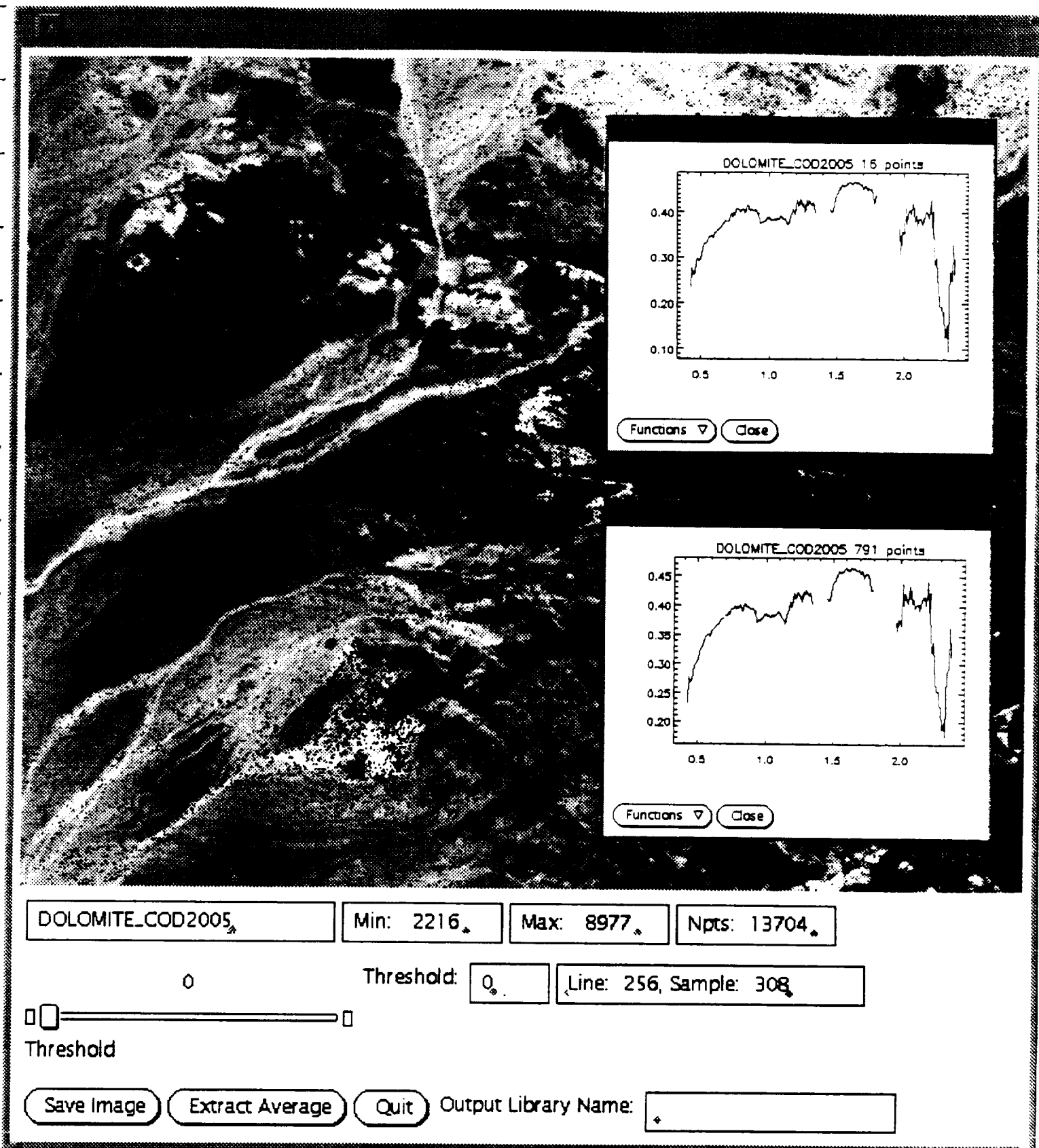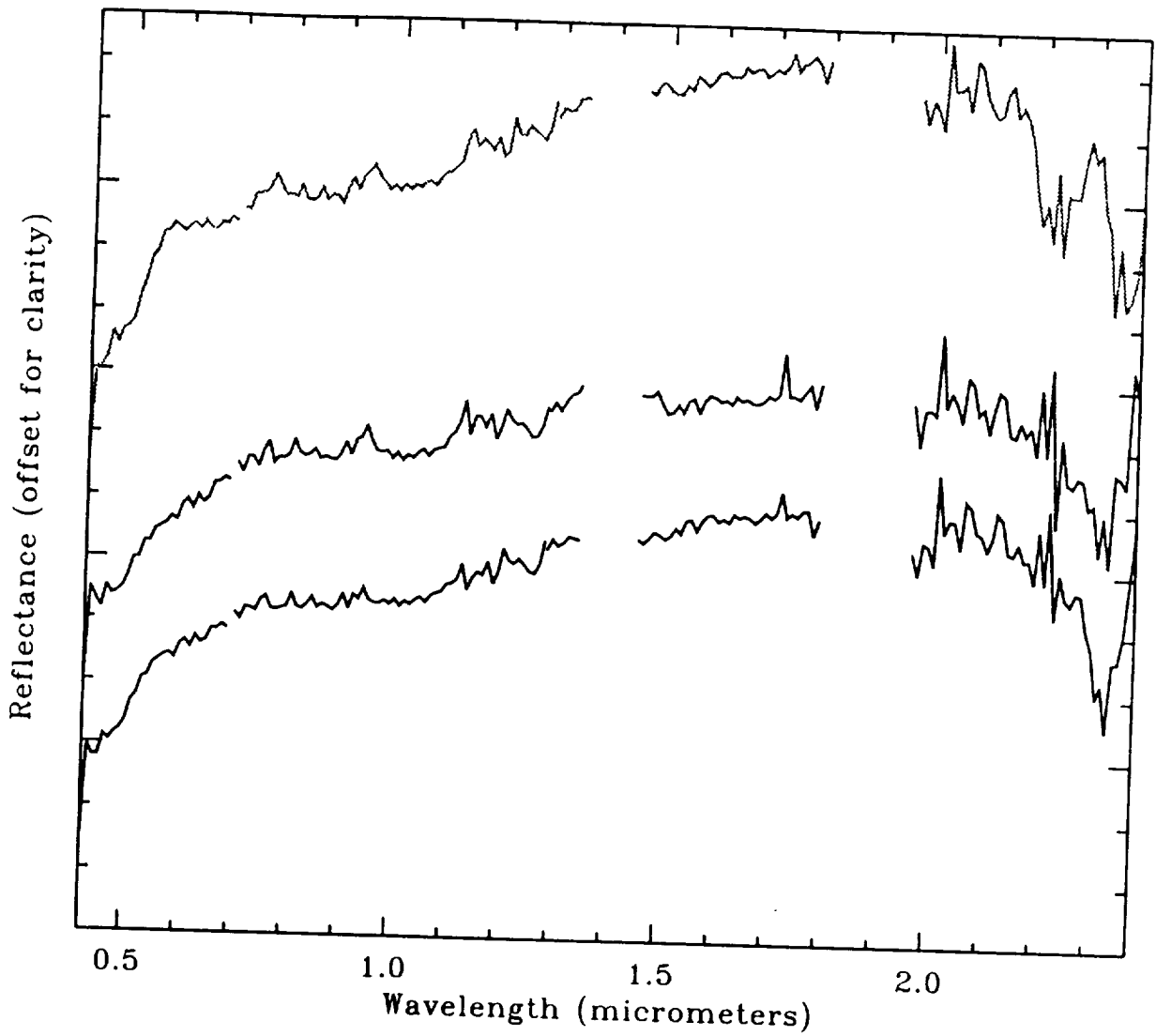mineral in the library at each pixel of the image. Individual images from this cube can be displayed and analyzed using graphically-based software tools to produce thematic image maps showing the distribution of materials at the surface. The results described here and other ongoing studies indicate that the expert system in its present state is a viable system for automated mineralogical mapping. Continued testing and refinement, and improvement of SNR characteristics of imaging spectrometers promise improved performance. Preliminary work with other materials indicates that these techniques should be extensible to areas other than mineralogy.

The feature extraction procedures and the expert system have been successfully used to analyze lab and field spectra of unknown materials and Airborne Visible/Infrared Imaging Spectrometer (AVIRIS) data. The expert system has successfully identified and mapped areas of the minerals kaolinite, alunite, and buddingtonite at one site using 63 channel imaging spectrometer data and areas containing the minerals hematite, goethite, sericite (fine grained muscovite), calcite, dolomite, halloysite, kaolinite, and alunite at other sites using the 224 channel AVIRIS data. The feature extraction and absorption band characterization procedures have been successfully tested on entire AVIRIS cubes.

It is clear that efficient use of automated techniques simplifies the task of extracting information from imaging spectrometer data. The expert system developed as the result of this research brings within reach automated, quantitative analysis of data sets such as AVIRIS.

V   RECOMMENDATIONS FOR FURTHER RESEARCH

This and similar research is important to the future of NASA'S imaging spectrometer program. One key point is the fact that this type of research is impossible without adequate spectral databases. Future efforts should concentrate on acquiring additional well-characterized high-spectral resolution measurements. Extension of the databases to include a variety of materials both naturally occurring and man-made is essential. This should also include detailed studies of spectral variability. Interdisciplinary studies involving scientists with spectral properties expertise for a variety of materials is recommended.

Further testing of the expert system capabilities is required. Merging the feature-based techniques with other noise-tolerant techniques should be of particular interest. This would require acquisition of additional imaging spectrometer data sets, implementation of new algorithms, and testing of the expert system for specific surface classes and conditions.

Finally, the expert system results demonstrate that operational imaging spectrometers such as AVIRIS are providing spectral data of sufficient quality to perform detailed quantitative mapping. Further improvement of these capabilities is dependent upon continued development and support of high quality imaging spectrometers providing data with near-laboratory-quality signal-to-noise ratios.

VI. REFERENCES CITED

Brindley, G., Suzuki, T., and Thiry, M., 1983. Interstratified kaolinite/smectites from the Paris Basin; correlation of layer proportions, chemical compositions, and other data: Bull. Minéral., v. 106, p. 403-410.

Chang, S. H., and Collins, W. E., 1983, Confirmation of the airborne biogeophysical mineral exploration technique using laboratory methods: Econ. Geol., v. 78, p. 723-736.

Clark, R. N., and Roush, T. L., 1984, Reflectance spectroscopy: Quantitative analysis techniques for remote sensing applications: Journal of Geophysical Research, v. 89, no. B7, pp. 6329-6340.

Clark, R. N., King, T. V. V., Klejwa, M., and Swayze, G. A., 1990, High spectral resolution spectroscopy of minerals: Journal of Geophysical Research, v. 95, no. B8, p. 12653-12680.

Collins, W. E., 1978, Remote sensing of crop type and maturity: Photogramm. Eng. Remote Sens., v. 44, no. 1, p. 43-55.

Curtiss B. and Ustin, S.L., Parameters effecting reflectance of coniferous forests in the region of chlorophyll absorption: Proceedings of IGARSS '89, 12th Canadian Symposium on Remote Sensing, Vancouver, British Columbia.

Gates, D. M., 1970, Physical and physiological properties of plants: in Remote Sensing with Special Reference to Agriculture and Forestry, Natl. Acad. Sci., Washington, D. C., p. 224-252.

Gates, D, M., Keegan, H. J., Schleter, J. D., and Weidner, V. R., 1965, Spectral properties of plants: Appl. Opt. v. 4, no. 1, p. 11-20.

Geophysical and Environmental Research, 1988, Single beam visible/InfraRed Intelligent Spectroradiometer (SIRIS) User's Manual, GER, Milbrook, N.Y.

Goetz, A. F. H., Vane, Gregg, Solomon, J. E., and Rock, B. N., 1985, Imaging spectrometry for earth remote sensing: Science, v. 228, p. 1147-1153.

Goetz, A. F. H., Gao, B. C., Wessman, C. A., and Bowman, W. D., 1990, Estimation of biochemical constituents from fresh, green leaves by spectrum matching techniques: in Proceedings International Geolscience and Remote Sensing Symposium, Remote Sensing Science for the Nineties (IGARSS ' 90), v. 2, p. 971-974.

Grove, C. I., Hook, S. J., and Paylor, E. D., 1992, Laboratory reflectance spectra of 160 minerals, 0.4 to 2.5 micrometers: JPL Publication 92-2.

Hauff, P. L., and Kruse, F. A., 1990, Spectral identification and characterization (1.2 - 2.5 μm) of kaolinite/smectite clays in weathering environments:

Proceedings, Australasian Remote Sensing Conference, 5th, Perth, Western Australia, p. 898 - 905.

Hauff, P. L., Kruse, F. A., and Thiry, M., 1990, Characterization of interstratified Kaolinite/smectite clays using infrared reflectance spectroscopy (1.2 - 2.5 μm): _Chemical Geology,_ v. 84, no. 1/4, July 5 1990, p. 267-270.

Hunt, G. R., 1977, Spectral signatures of particulate minerals in the visible and near-infrared: _Geophysics,_ v. 42, no. 3, p. 501-513.

Hunt, G. R., 1979, Near-infrared (1.3-2.4μm) spectra of alteration minerals - potential for use in remote sensing: _Geophysics,_ v. 44, p. 1974-1986.

Hunt, G. R., and Ashley, R. P., 1979, Spectra of altered rocks in the visible and near infrared: _Econ. Geol.,_ v. 74, p. 1613-1629.

Hunt, G. R., and Salisbury, J. W., 1970, Visible and near-infrared spectra of minerals and rocks: II. Carbonates: _Mod. Geol.,_ v. 2, p. 23-30.

Hunt, G. R., Salisbury, J. W., and Lenhof, C. J., 1971, Visible and near-infrared spectra of minerals and rocks: III. Oxides and hydroxides: _Mod. Geol.,_ v. 2, p. 195-205.

Joint Committee on Powder Diffraction Standards (JCPDS), 1974, Selected powder diffraction data for minerals: _compiled by the JCPDS--International Centre for Diffraction Data in cooperation with the American Society for Testing and Materials (et al.),_ Swarthmore, Pa., 3 volumes.

Joint Committee on Powder Diffraction Standards (JCPDS), 1980, Selected powder diffraction data for minerals, data book, Supplement: _compiled by the JCPDS--International Centre for Diffraction Data in cooperation with the American Society for Testing and Materials (et al.),_ Swarthmore, Pa.

Knipling, E. B., 1970, Physical and physiological basis for the reflectance of visible and near-infrared radiation from vegetation: _Remote Sensing of Environment,_ v. 1, p. 155-159.

Kruse, F. A., 1988, Use of Airborne Imaging Spectrometer data to map minerals associated with hydrothermally altered rocks in the northern Grapevine Mountains, Nevada and California: _Remote Sensing of Environment, Special issue on imaging spectrometry,_ V. 24, No. 1, p. 31-51.

Kruse, F. A., Calvin, W. M., and Seznec, O., 1988, Automated extraction of absorption features from Airborne Visible/Infrared Imaging Spectrometer (AVIRIS) and Geophysical Environmental Research imaging spectrometer (GERIS) data: In Proceedings of the Airborne Visible/Infrared Imaging Spectrometer (AVIRIS) performance evaluation workshop, _JPL Publication 88-38,_ p. 62-75.

57

Kruse, F. A. and Hauff, P. L., 1989, Identification of illite polytype zoning in disseminated gold deposits using reflectance spectroscopy and X-ray diffraction -- Potential for mapping with imaging spectrometers: *in* Proceedings, IGARSS '89, 12th Canadian Symposium on Remote Sensing, v. 2, p 965-968.

Kruse, F. A., Seznec, O., and Krotkov, P. M., 1990a, An expert system for geologic mapping with imaging spectrometers: in Proceedings, Applications of Artificial Intelligence VIII, Society of Photo-Optical Instrumentation Engineers (SPIE), v. 1293, p. 904-917.

Kruse, F. A., Kierein-Young, K. S., and Boardman, J. W., 1990b, Mineral mapping at Cuprite, Nevada with a 63 channel imaging spectrometer: Photogrammetric Engineering and Remote Sensing, v. 56, no. 1, p. 83-92.

Kruse, F. A., 1990a, Artificial Intelligence for Analysis of Imaging Spectrometer Data: Proceedings, ISPRS Commission VII, Working Group 2: "Analysis of High Spectral Resolution Imaging Data", Victoria, B. C., Canada, 17-21 September, 1990, p. 59-68.

Kruse, F. A., 1990b, Thematic mapping with an expert system and imaging spectrometers: Proceedings, ISPRS Commission II/VIII International Workshop on "Advances in spatial information extraction and analysis for Remote Sensing": American Society for Photogrammetry and Remote Sensing, Bethesda, MD, p. 59-68.

Kruse, F. A. and Hauff, P. L., 1991, Identification of illite polytype zoning in disseminated gold deposits using reflectance spectroscopy and X-ray diffraction -- Potential for mapping with imaging spectrometers: IEEE Transactions on Geoscience and Remote Sensing, v. 29, no. 1, p. 101-104.

Kruse, F. A., Thiry, M., and Hauff, P. L., 1991, Spectral identification (1.2 - 2.5 µm) and characterization of Paris Basin kaolinite/smectite clays using a field spectrometer: in Proceedings of the Cinquième Colloque International, Mesures Physiques et Signatures En Télédétection, 14 - 18 January 1991, Courchevel, France, European Space Agency, esa SP-319, v. 1, p. 181-184.

Kruse, F. A., 1992a, Expert System-Based Mineral Mapping Using AVIRIS: In Summaries of the Third Annual JPL Airborne Geoscience Workshop, AVIRIS Workshop, JPL Publication 92-14, V. 1, p. 119 - 121.

Kruse, F. A., 1992b, Prototyping HIRIS analysis techniques using AVIRIS data: Final Report, U. S. Geological Survey Cooperative Agreement 14-08-0001-A0746, CSES/CIRES, University of Colorado, Boulder CO, 25 p.

Kruse, F. A., and Lefkoff, A. B., 1992, Hyperspectral imaging of the Earth's surface - an expert system-based analysis approach: *in* Proceedings of the International

Symposium on Spectral Sensing Research, 15 - 20 November 1992, Mauii, Hawaii, (in press).

Kruse, F. A., and Lefkoff, A. B., 1993, Knowledge-based geologic mapping with imaging spectrometers: Remote Sensing Reviews, Special Issue on NASA Innovative Research Program (IRP) results, (in press).

Kruse, F. A., Lefkoff, A. B., and Dietz, J. B., 1993a, Expert System-Based Mineral Mapping in northern Death Valley, California/Nevada using the Airborne Visible/Infrared Imaging Spectrometer (AVIRIS): Remote Sensing of Environment, Special issue on AVIRIS (in press).

Kruse, F. A., Lefkoff, A. B., Boardman, J. B., Heidebrecht, K. B., Shapiro, A. T., Barloon, P. J., and Goetz, A. F. H., 1993b, The Spectral Image Processing System (SIPS) - Interactive Visualization and Analysis of Imaging Spectrometer Data: Remote Sensing of Environment, Special issue on AVIRIS (in press).

Kruse, F. A., and Hauff, P. L., (eds.), 1993, The IGCP-264 Spectral Properties Database: AGU Special Publication, 211 p. (in press)

Lee, Keenan, and Raines, G. L., 1984, Reflectance spectra of some alteration minerals- -a chart compiled from published data 0.4μm-2.5μm: U.S. Geological Survey Open-File Report 84-96, 6 p., 1 chart.

Lucas, J., Trauth, N., and Thiry, M., 1974, Les minéraux argileux des sédiments paléogènes du bassin de Paris - Evolution des smectites et des interstratifiés (7-14Sm): Bull. Gr. Fr. Argiles, v. 24, p. 245-262.

Mazer, A. S.,Martin, Miki, Lee, Meemong, and Solomon, J. E., 1988, Image processing software for imaging spectrometry data analysis: Remote Sensing of Environment, v. 24, no. 1, p. 201-210.

Peterson, D. L., Aber, J. D., Matson, P. A., Card, D. H., Swanberg, N., Wessman, C., and Spanner, M., 1988, Remote sensing of forest canopy and leaf biochemical contents: Remote Sensing of Environment, Special issue on imaging spectrometry, V. 24, No. 1, p. 85-108.

Pieters, C. M., 1990, Reflectance Experiment Laboratory Description and User's Manual , RELAB, Brown University, Providence, RI.

Porter, W. M., and Enmark, H. T., 1987 A system overview of the Airborne Visible/Infrared Imaging Spectrometer (AVIRIS): in Proceedings, 31st Annual International Technical Symposium, Society of Photo-Optical Instrumentation Engineers, v. 834, pp. 22-31.

Quintus Computer Systems, 1987, QUINTUS PROLOG Reference Manual, Version 10, Quintus Computer Systems, Mountain View, CA.

Research Systems, Inc., (RSI), 1992, IDL® User's Guide Version 3.0, Research Systems, Inc., Boulder, Colorado.

Reynolds, R. C., 1980, Interstratified clay minerals: *in* Crystal structures of clay minerals and their X-Ray identification, Brindley, G. W., and Brown, G. (eds.), Mineral. Soc. of London, Ch 4. p. 249-303.

Rock, B. N., 1988, Comparison of in-situ and airborne spectral measurements of the blue shift associated with forest decline: Remote Sensing of Environment, v. 24, p. 109-127.

Salisbury, F. B. and Ross, C., 1969, Plant Physiology, Wadsworth, San Francisco, CA, p. 262-265.

Schultz, L. G., Shepard, A. O., Blackmon, P. D., and Starkey, H. C., 1971, Mixed layer kaolinite-montmorillonite from the Yucatan Peninsula, Mexico: Clays and Clay Minerals, v. 19, p. 137-150.

Shimoyama, B. A., Johns W. D., and Sudo, T., 1969, Montmorillonite-kaolinite clay in acid clay deposits from Japan: International Clay Conference, 1st, Tokyo, p.225-231.

Singhroy, V.H., and Kruse, F.A. 1991, "Detection of Metal Stress in Boreal Forest Species Using the 0.67 Micrometer Chlorophyll Absorption Band", Erim Thematic Conf., Proc., 8th, Geologic Remote Sensing, Exploration, Engineering, and Environment Denver, CO, Erim Ann Arbor, MI., pp. 361-372

Thiry, M., 1989, The Argiles Plastiques Formation of the Paris Basin: Continental clay deposits and paleoweathering: *in* Guide Book, Post-Congress Field-Trip IV-V, 9th International Clay Conference, Assoc. Intern. pour L'Étude des argiles, p. 3-16.

Thomas, J., and Oerther, G., 1972, Leaf reflectance v. leaf chlorophyll and carotenoid concentrations for eight crops: Agron. J., v. 64, p. 799-807.

Tsay, M. L., Gjerastad, D. H., and Glover, G. R., 1982, Tree leaf reflectance: A promising technique to rapidly determine nitrogen and chlorophyll content: Can. J. For. Res., v. 12, p.788.

Ustin, S. L., and Curtiss, B., 1989, Early detection of air pollution injury to coniferous forests using remote sensing: National Council of the Paper Industry for Air and Stream Improvement (NCASI) Technical Bulletin No. 571: NCASI, New York, NY, 25 p.

Wiewiora, A., 1971, A mixed-layer kaolinite-smectite from Lower Silesia, Poland: Clays and Clay Minerals, v. 19, p. 415-416.

Wilson, M. J., and Gradwick, P. D., 1972, Occurrence of interstratified kaolinite-montmorillonite in some Scottish soils: Clays and Clay Minerals, v. 9, p. 435-437.

Yerima, B. P. K., Calmoun, F. G., Senkaji, A. L., and Dixon, J. B., 1985, Occurrence of interstratified kaolinite-smectite in Salvador Vertisols: Soil Sc. Soc. Am. J., v. 49, p. 462-466.

APPENDIX A   PUBLICATIONS LIST OF RESEARCH SUPPORTED OR PARTIALLY SUPPORTED BY NAGW-1601 (1989-1993)

PEER REVIEWED JOURNAL PAPERS

Kruse, F. A., and Lefkoff, A. B., 1993, Knowledge-based geologic mapping with imaging spectrometers: Remote Sensing Reviews, Special Issue on NASA Innovative Research Program (IRP) results, (in press).

Kruse, F. A., Lefkoff, A. B., and Dietz, J. B., 1993, Expert System-Based Mineral Mapping in northern Death Valley, California/Nevada using the Airborne Visible/Infrared Imaging Spectrometer (AVIRIS): Remote Sensing of Environment, Special issue on AVIRIS (in press).

Kruse, F. A., Lefkoff, A. B., Boardman, J. B., Heidebrecht, K. B., Shapiro, A. T., Barloon, P. J., and Goetz, A. F. H., 1993, The Spectral Image Processing System (SIPS) - Interactive Visualization and Analysis of Imaging Spectrometer Data: Remote Sensing of Environment, Special issue on AVIRIS (in press).

Kruse, F. A. and Hauff, P. L., 1991, Identification of illite polytype zoning in disseminated gold deposits using reflectance spectroscopy and X-ray diffraction -- Potential for mapping with imaging spectrometers: IEEE Transactions on Geoscience and Remote Sensing, v. 29, no. 1, p. 101-104.

Kruse, F. A., and Hauff, P. L., 1990, Remote sensing clay mineral investigations for geologic applications using visible/near-infrared imaging spectroscopy: Sciences Géologiques, Mémoir No. 89, p. 43-51.

Hauff, P. L., Kruse, F. A., and Thiry, M., 1990, Characterization of interstratified Kaolinite/smectite clays using infrared reflectance spectroscopy (1.2 - 2.5 µm): Chemical Geology, v. 84, no. 1/4, July 5 1990, p. 267-270.

Kruse, F. A., Kierein-Young, K. S., and Boardman, J. W., 1990, Mineral mapping at Cuprite, Nevada with a 63 channel imaging spectrometer: Photogrammetric Engineering and Remote Sensing, v. 56, no. 1, p. 83-92.

PEER REVIEWED SPECIAL PUBLICATIONS

Kruse, F. A., and Hauff, P. L., (eds.), 1993, The IGCP-264 Spectral Properties Database: AGU Special Publication, 211 p., (in press).

PROCEEDINGS PAPERS

Kruse, F. A., and Lefkoff, A. B., 1992, Hyperspectral imaging of the Earth's surface - an expert system-based analysis approach: in Proceedings of the International Symposium on Spectral Sensing Research, 15 - 20 November 1992, Mauii, Hawaii, (in press).

Kruse, F. A., 1992, Geologic Remote Sensing - New Technology, New Information: in Proceedings, IGARSS'92, 26-29 May, 1992, Houston, Tx, IEEE Catalog Number 92CH3041-1, V. 1, p. 625 - 627.

Kruse, F. A., Lefkoff, A. B., Boardman, J. B., Heidebrecht, K. B., Shapiro, A. T., Barloon, P. J., and Goetz, A. F. H., 1992, The Spectral Image Processing System (SIPS) - Software for Integrated Analysis of AVIRIS Data: In Summaries of the Third Annual JPL Airborne Geoscience Workshop, Volume 1, AVIRIS Workshop, JPL Publication 92-14, p. 23 - 25.

Kruse, F. A., 1992, Expert System-Based Mineral Mapping Using AVIRIS: In Summaries of the Third Annual JPL Airborne Geoscience Workshop, AVIRIS Workshop, JPL Publication 92-14, V. 1, p. 119 - 121.

Kruse, F. A., Lefkoff, A. B., Boardman, J. B., Heidebrecht, K. B., Shapiro, A. T., Barloon, P. J., and Goetz, A. F. H., 1992, The Spectral Image Processing System (SIPS) - Interactive analysis of hyperspectral

images: in Proceedings, International Space Year Conference on Earth and Space Science Information Systems: February 10-13, 1992, Pasadena, California.

Kruse, F. A., Dietz J. B., and Kierein-Young, K. S., 1991, (Extended Abst.), Geologic Mapping in Death Valley, California/Nevada Using NASA/JPL Airborne Systems (AVIRIS, TIMS, and AIRSAR): In Proceedings of the 3rd Airborne Visible/Infrared Imaging Spectrometer (AVIRIS) workshop, JPL Publication 91-28, p. 258-259

Kruse, F. A., Thiry, M., and Hauff, P. L., 1991, Spectral identification (1.2 - 2.5 μm) and characterization of Paris Basin kaolinite/smectite clays using a field spectrometer: in Proceedings of the Cinquième Colloque International, Mesures Physiques et Signatures En Télédétection, 14 - 18 January 1991, Courchevel, France, European Space Agency, esa SP-319, v. 1, p. 181-184.

Singhroy, V. H., and Kruse, F. A., 1991, Detection of metal stress in boreal forest species using the 0.67 μm chlorophyll absorption band: in Proceedings, International Symposium on Remote Sensing of Environment, Thematic Conference on Remote Sensing for Exploration Geology, 8th, 29 April - 2 May 1991, Denver, Colorado, Environmental Research Institute of Michigan, Ann Arbor, p. 361 - 372.

Kruse, F. A., 1990, Artificial Intelligence for Analysis of Imaging Spectrometer Data: Proceedings, ISPRS Commission VII, Working Group 2: "Analysis of High Spectral Resolution Imaging Data", Victoria, B. C., Canada, 17-21 September, 1990, p. 59-68.

Kruse, F. A., 1990, Thematic mapping with an expert system and imaging spectrometers: Proceedings, ISPRS Commission II/VIII International Workshop on "Advances in spatial information extraction and analysis for Remote Sensing": American Society for Photogrammetry and Remote Sensing, Bethesda, MD, p. 59-68.

Kruse, F. A., 1990, Identification and mapping of alteration minerals with the Airborne Visible/Infrared Imaging Spectrometer (AVIRIS): Proceedings, Australasian Remote Sensing Conference, 5th, Perth, Western Australia, p. 146-154.

Kruse, F. A., 1990, Analysis of Airborne Visible/Infrared Imaging Spectrometer (AVIRIS) data for the northern Death Valley region, California and Nevada: In Proceedings of the 2nd Airborne Visible/Infrared Imaging Spectrometer (AVIRIS) workshop, 4-5 June 1990, JPL Publication 90-54, p. 100-106.

Hauff, P. L., and Kruse, F. A., 1990, Spectral identification and characterization (1.2 - 2.5 μm) of kaolinite/smectite clays in weathering environments: Proceedings, Australasian Remote Sensing Conference, 5th, Perth, Western Australia, p. 898 - 905.

Kruse, F. A., Seznec, O., and Krotkov, P. M., 1990, An expert system for geologic mapping with imaging spectrometers: in Proceedings, Applications of Artificial Intelligence VIII, Society of Photo-Optical Instrumentation Engineers (SPIE), v. 1293, p. 904-917.

Hauff, P. L., and Kruse, F. A., 1990, Defining gold ore-zones using illite polytypes: in Proceedings, Geology and ore deposits of the Great Basin, 1-5 April, 1990, Sparks, Nevada.

Kruse, F. A. and Hauff, P. L., 1989, Identification of illite polytype zoning in disseminated gold deposits using reflectance spectroscopy and X-ray diffraction -- Potential for mapping with imaging spectrometers: in Proceedings, IGARSS '89, 12th Canadian Symposium on Remote Sensing, v. 2, p 965-968.

Kruse, F. A., and Taranik, D. L., 1989, Mapping hydrothermally altered rocks with the Airborne Imaging Spectrometer (AIS) and the Airborne Visible/Infrared Imaging Spectrometer (AVIRIS): in Proceedings, IGARSS '89, 12th Canadian Symposium on Remote Sensing, v. 2, p 952-956.

Kruse, F. A., and Kierein-Young, K. S., 1989, Analysis of Geophysical and Environmental Research Imaging Spectrometer (GERIS) data for the Cuprite Mining District, Esmeralda and Nye Counties, Nevada: Proceedings, Image Processing '89, Reno, Nevada, p. 56 - 65.

Hauff, P. L., Kruse, F. A., and Madrid, R. J., 1989, Gold exploration using illite polytypes defined by X-Ray diffraction and reflectance spectroscopy: in Proceedings, Gold Forum on Technology and Practices, "World Gold '89", Society for Mining, Metallurgy, and Exploration, Littleton, Colorado, p. 76-82.

IN-HOUSE REPORTS

Lefkoff, A. B., and Kruse, F. A., 1993, General Use Expert System for Spectra (GUESS) User's Guide, Version 1.0, Center for the Study of Earth from Space (CSES), 25 p.

Center for the Study of Earth from Space (CSES), 1991, SIPS User's Guide, Spectral Image Processing System Version 1.0, 90 p.

Center for the Study of Earth from Space (CSES), 1992, SIPS User's Guide, Spectral Image Processing System Version 1.1, 79 p.

Center for the Study of Earth from Space (CSES), 1992, SIPS User's Guide, Spectral Image Processing System Version 1.2, 88 p.

Kruse, Fred A., 1992, Prototyping HIRIS analysis techniques using AVIRIS data: Final Report, U. S. Geological Survey Cooperative Agreement 14-08-0001-A0746, CSES/CIRES, University of Colorado, Boulder CO, 25 p.

TRADE JOURNALS

Kruse, F. A., 1992, The analysis of scientific data from NASA airborne systems: Scientific Computing & Automation, June 1992, Elsevier, p. 15-22.

ABSTRACTS

Kruse, F. A., and Lefkoff, A. B., 1992, Hyperspectral imaging of the Earth's surface: in Abstracts Digest, International Symposium on Spectral Sensing Research, 15 - 20 November 1992, Mauii, Hawaii, p. 74.

Kruse, F. A., 1992, Mapping of mineral deposits using remote sensing techniques (Abst.): in Book of Abstracts, The World Space Congress, 29th Plenary Meeting of the Committee on Space Research (COSPAR), Washington, D. C., 28 Aug - 5 Sept 1992, p. 292.

Kruse, F. A., 1991, Imaging Spectrometry - A new technology for improved geologic mapping (Abst.): in Abstract Volume, 5th Meeting, IGCP-264, Remote Sensing Spectral Properties, 2-12 December 1991, Department of Geology, University of Poona, Pune, India, p. 64.

Thiry, M., Hauff, P. L., and Kruse, F. A., 1991, Evolutions récentes des techniques de spectrométrie Infra-Rouge en télédétection et application aux minéraux argileux: in Proceedings, Reunion du 21 mars 1991 du Goupe Francais des Argiles, Paris, France.

Hauff, P. L., and Kruse, F. A., 1990, Defining gold ore-zones using illite polytypes (Abst.): in Proceedings, Geology and ore deposits of the Great Basin, 1-5 April, 1990, Sparks, Nevada.

Hauff, P. L., Kruse, F. A., Bakken, B. M., and Madrid. R., 1989, (Abst.) Using illite polytypes and illite crystallinity to characterize gold deposits -- From megascopic to microscopic perspectives: 9th International Clay Conference, Association Internationale Pour l'Etude des Argiles, 28 August-2 September, 1989, Strasbourg, France, p. 173.

Kruse, F. A., 1989, (Abst.), Remote sensing clay mineral investigations for geologic applications using visible/near-infrared imaging spectroscopy: 9th International Clay Conference, Association Internationale Pour l'Etude des Argiles, 28 August-2 September, 1989, Strasbourg, France, p. 219.

Hauff, P. L., and Kruse, F. A., 1989, Gold exploration using illite polytypes defined by X-Ray diffraction and reflectance spectroscopy (Abst.): in Program with abstracts, World Gold '89.

Kruse, F. A., 1989, Mineralogical mapping with imaging spectroscopy for precious metals exploration (Abst.): in Summaries, International Symposium on Remote Sensing of Environment, Thematic Conference on Remote Sensing for Exploration Geology, 7th, 2-6 October, 1989, Calgary, Alberta, Canada, Environmental Research Institute of Michigan, Ann Arbor.